arXiv:1210.3016v1 [hep-th] 10 Oct 2012

Refined Topological Strings and Toric Calabi-Yau Threefolds

Amer Iqbal,♠ **Can Kozçaz,**♣,[1]

♠Department of Physics, LUMS School of Science & Engineering, U-Block, D.H.A, Lahore, Pakistan.

♠Department of Mathematics, LUMS School of Science & Engineering, U-Block, D.H.A, Lahore, Pakistan.

♣PH-TH Division, CERN, Genève, CH-1211 Switzerland.

♣International School of Advanced Studies (SISSA), via Bonomea 265, 34136 Trieste, Italy and INFN, Sezione di Trieste

E-mail: amer.iqbal@lums.edu.pk, Can.Kozcaz@sissa.it

ABSTRACT: The refined topological vertex formulation computes the refined topological string partition function for non-compact toric Calabi-Yau threefolds which engineer $\mathcal{N}=2$ supersymmetric gauge theories. For geometries such as the local $\mathbf{P}^2$, which do not give rise to gauge theories, the refined topological vertex alone is not sufficient for directly calculating the refined amplitudes. In this paper, we extend the refined topological vertex formalism and propose a complementary new vertex which, together with the refined topological vertex, determines the refined amplitudes for all toric Calabi-Yau threefolds.

---

[1] Current affiliation SISSA

Contents

1 Introduction **1**

2 The refined vertex and gauge theory **3**

3 The case of local $\mathbf{P}^2$ **8**
3.1 The refinement of local $\mathbf{P}^2$ 10

4 The New Refined Vertex **13**
4.1 Derivation of the two-legged new vertex 15
4.2 The new vertex 19

5 Gluing Rules for the New Vertex with the Refined Topological Vertex **21**

6 Applications of the new vertex **23**
6.1 Example 1: $\mathcal{O}_{\mathbf{P}^1}(-1) \oplus \mathcal{O}_{\mathbf{P}^1}(-1)$ 23
6.2 Example 2: Local $\mathbf{P}^1 \times \mathbf{P}^1$ 24
6.3 Example 3: Local $\mathbf{F_1}$ 24
6.4 Example 4 25

7 Relation with refined Chern-Simons theory **26**
7.1 Local $\mathbf{P}^2$ from refined Chern-Simons Theory 27

8 Conclusions **29**

9 Appendix A **30**

10 Appendix B **32**

1 Introduction

The topological string theory amplitudes are useful in the study of the BPS sector of the string compactifications. $\mathcal{N} = 2$ topological strings on Calabi-Yau threefolds capture the quantum numbers of the BPS states obtained by wrapping branes on holomorphic curves [1]. When the Calabi-Yau threefold is non-compact, the topological string amplitudes completely determine the prepotential, and the higher genus corrections to it, of the gauge theory which lives in the spacetime [2]. Surprisingly these amplitudes also determine the superconformal index of the 5D superconformal theories which appear by M-theory compactification on non-compact Calabi-Yau threefolds [3].

Advances in the instanton computation of $\mathcal{N}=2$ gauge theories motivated the refinement of the topological string amplitudes for non-compact Calabi-Yau threefolds [2, 4, 5] . From the target space interpretation of the topological string theory the refinement corresponds to an explicit determination of the quantum numbers of BPS particles in M-theory compactifications on the same Calabi-Yau threefold [1, 5] with respect to the $SO(4)=SU(2)_L\times SU(2)_R$ part of the 5D Lorentz group. Therefore it is particularly useful to be able to calculate these refined amplitudes for a non-compact Calabi-Yau threefold. The topological vertex completely solved the problem of determining the usual topological string amplitudes for non-compact toric Calabi-Yau threefolds [6]. The refined topological vertex formulation extends the usual one and calculates the refined amplitudes for a certain class of non-compact toric Calabi-Yau threefolds [7]. The class of Calabi-Yau threefolds for which the refined vertex formalism works includes the geometries giving rise to gauge theory in spactime when type IIA strings are compactified on these Calabi-Yau threefolds. However, there exist toric Calabi-Yau threefolds which do not give rise to a gauge theory, such as the local $\mathbf{P}^2$, and the refined topological vertex formalism can not be applied to such geometries directly[1].

In this note, we introduce a complementary topological vertex, $T_{\lambda\,\mu\,\nu}(t,q)$, which together with the refined topological vertex extends the formalism to all non-compact toric Calabi-Yau threefolds. We believe that this new vertex is closely related to the "index vertex" of Okounkov and Nekrasov [8].

The paper is organized as follows: in section 2, we discuss the origin of the refined topological vertex, its relation with instanton calculus of 4D gauge theory and the appearance of a preferred direction. In section 3, we discuss the case of local $\mathbf{P}^2$ and show the need for a new vertex. In this section we also calculate the refined partition function of the local $\mathbf{P}^2$. In section 4, we calculate the new vertex. Section 5 is reserved to the gluing rules of the new topological vertex with the refined topological vertex. We argue how the new vertex together with the refined vertex completely solve the problem of calculating the refined amplitudes for toric Calabi-Yau threefolds. In section 6, we give some applications of the new vertex. In section

---

[1] However, BPS multiplicities can be calculated by appropriately identifying the curves that survive the blow down from a larger geometry, to which refined vertex formalism can be applied, in which it can be embedded. For local $\mathbf{P}^2$ the BPS multiplicities were calculated in [7]

7, we discuss the relation of our approach to the refined Chern-Simons theory. Some technical points are included in appendix A. Notation and identities used are given in appendix B.

2 The refined vertex and gauge theory

The geometric engineering provides a beautiful link connecting the spacetime physics with the geometry of the Calabi-Yau threefold. Type IIA strings compactified on Calabi-Yau threefolds give rise to $\mathcal{N}=2$ theory on the spacetime. The prepotential of the $\mathcal{N}=2$ theory on the spacetime is given by the genus zero amplitude of the topological strings propagating on the Calabi-Yau threefold. The higher genus amplitudes of the Calabi-Yau threefold appear when the gauge theory is coupled with gravity and, in case spacetime theory is a gauge theory coming from a toric Calabi-Yau threefold, can be calculated using the instanton calculus [2]. The Kähler parameters of the Calabi-Yau geometry are related, on the gauge theory side, to the expectation values of scalars in the vector multiplet $\vec{\mathbf{a}}$, the mass of the hypermultiplets and the gauge couplings. The string coupling constant is given by the equivariant parameter of the $U(1)$ action on $\mathbb{C}^2$:

$$(z_1, z_2) \in \mathbb{C}^2 \mapsto (q\, z_1, q^{-1}\, z_2)\,, \quad q = e^{i\epsilon}\,. \tag{2.1}$$

This $U(1)$ action lifts to an action on the instanton moduli spaces with isolated fixed points labelled by the partitions of the instanton charge. For the $SU(N)$ gauge group the isolated fixed points of the k instanton moduli space are labelled by N partitions $\{Y_1, Y_2, \cdots, Y_N\}$ such that $\sum_a |Y_a| = k$, where $Y_a = \{Y_{a,1} \geq Y_{a,2} \geq Y_{a,3} \geq \cdots \,|Y_{a,i} \in \mathbb{Z}_{\geq 0}\}$ and $|Y_a| = \sum_i Y_{a,i}$. The instanton partition function is given by

$$Z_{instanton} = \sum_{k=0}^{\infty} Q^k\, Z_k(\vec{\mathbf{a}}, \epsilon) = \sum_{Y_1, Y_2, \cdots, Y_N} Q^{|Y_1|+Y_2|+\cdots+|Y_N|}\, Z_{Y_1, Y_2, \cdots, Y_N}(\vec{\mathbf{a}}, \epsilon), \tag{2.2}$$

where $Z_{Y_1,Y_2,\cdots,Y_N}$ is the contribution from the fixed point labelled by $\{Y_1, Y_2, \cdots, Y_N\}$

$$Z_{Y_1,Y_2,\cdots,Y_N}(\vec{\mathbf{a}}, \epsilon) = \prod_{a,b=1}^{N} N_{Y_a, Y_b}(\mathbf{a}, \epsilon), \tag{2.3}$$

$$N_{Y_a, Y_b} = \left[\prod_{(i,j)\in Y_a} \left(1 - e^{i(\alpha_a - \alpha_b)} q^{Y^t_{b,j} + Y_{a,i} - i - j + 1}\right)\left(1 - e^{i(\alpha_a - \alpha_b)}\, q^{-Y^t_{a,j} - Y_{b,i} + i + j - 1}\right)\right]^{-1}.$$

The full partition function also includes the perturbative part Z_{pert}[2]

$$Z_{pert} = \left[\prod_{1 \le a < b \le N} \left(1 - e^{i(\alpha_a - \alpha_b)} q^i\, t^{j-1}\right) \left(1 - e^{i(\alpha_a - \alpha_b)} q^{i-1}\, t^j\right) \right]^{-1} . \tag{2.4}$$

The geometric engineering relates the full partition function of the gauge theory

$$Z(Q, \vec{\mathbf{a}}, \epsilon) = Z_{pert}(\vec{\mathbf{a}}, \epsilon) \times Z_{instanton}(Q, \vec{\mathbf{a}}, \epsilon)$$

with the partition function of topological strings propagating on a Calabi-Yau threefold [9]. In the case of the pure $\mathcal{N} = 2$ $SU(N)$ gauge theory we are discussing the Calabi-Yau threefold is the A_{N-1} geometry fibered over a $\mathbf{P}^1$. The BPS particles in the theory are given by branes wrapping various cycles in the Calabi-Yau threefold [10]. The k instanton contribution to the gauge theory partition function comes from worldsheet instanton wrapping k times the base $\mathbf{P}^1$ and arbitrary wrapping on the fiber $\mathbf{P}^1$'s of the A_{N-1} fiber. The partition function encodes the BPS spin content of the particles coming from wrapping M2-branes on holomorphic curves. In the M-theory compactification on the Calabi-Yau threefold each BPS particle has a mass equal to the area of the curve and has $SO(4) = SU(2)_L \times SU(2)_R$ quantum numbers which we denote by (j_L, j_R). The partition function is then given by [1]

$$Z = \prod_{\beta \in H_2(X,\mathbb{Z})} \prod_{k_L = -j_L}^{+j_L} \prod_{m=1}^{\infty} \left(1 - Q_\beta\, q^{2k_L + m}\right)^{(-1)^{2j_L+1} m\, N_\beta^{j_L}} , \tag{2.5}$$

where $Q_\beta = e^{-\int_\beta \omega}$ (ω being the complexified Kähler class) and

$$N_\beta^{j_L} = \sum_{j_R} (-1)^{2j_R} N_\beta^{j_L, j_R} , \tag{2.6}$$

$N_\beta^{j_L, j_R}$ being the number of particles with charge β and spin (j_L, j_R).

The refinement of topological strings was motivated by the fact that the equivariant localization computation mentioned above can also be carried out using the $U(1) \times U(1)$ action on $\mathbb{C}^2$

$$(z_1, z_2) \mapsto (q\, z_1, t^{-1}\, z_2) , \quad (q, t) = (e^{i\epsilon_1}, e^{-i\epsilon_2}), \tag{2.7}$$

in which case the gauge theory partition function depends on ϵ_1 and ϵ_2. The fixed points of the instanton moduli space under this action are still as before. The only difference being that N_{Y_a,Y_b} now depend on both q and t [2, 11],

---

[2] $\sum_{a=1}^{N} \alpha_a = 0$

$$N_{Y_a\,,Y_b} = \left[\prod_{(i,j)\in Y_a}\left(1-e^{i(\alpha_a-\alpha_b)}t^{Y^t_{b,j}-i}\,q^{Y_{a,i}-j+1}\right)\left(1-e^{i(\alpha_a-\alpha_b)}\,t^{-Y^t_{a,j}+i-1}\,q^{-Y_{b,i}+j}\right)\right]^{-1}.$$

Once the condition on the equivariant parameters is waived the general expansion defines the refinement of the topological string partition function. This is called refinement since it couples to the individual degenaracies with respect to the left-right spins [5],

$$Z_{refined} = \prod_{\beta\in H_2(X,\mathbb{Z})}\prod_{k_L=-j_L}^{+j_L}\prod_{k_R=-j_R}^{+j_R}\prod_{m_1,m_2=1}^{\infty}\left(1-Q_\beta\,t^{k_L-k_R+m_1-\frac{1}{2}}q^{k_L+k_R+m_2-\frac{1}{2}}\right)^{M_\beta^{j_L,j_R}}, \tag{2.8}$$
$$M_\beta^{j_L,j_R} = (-1)^{2j_L+2j_R}\,N_\beta^{j_L,j_R}.$$

The refinement has been studied both from the A-model side as well as the B-model point of view [5, 7, 12–17]. On the A-model side the refined topological vertex provides a powerful method for calculating the open and the closed partition functions for a certain class of toric Calabi-Yau threefolds [7]. The geometries for which the refined vertex formalism can be used are essentially those which give rise to $\mathcal{N}=2$ gauge theories in four dimensions via geometric engineering. Some simple Calabi-Yau threefolds such as local $\mathbf{P}^2$ (total space of $\mathcal{O}(-3)$ bundle on $\mathbf{P}^2$) do not give rise to gauge theory upon type IIA compactification. It is not possible to directly use the refined topological vertex formalism to write down the partition function for this Calabi-Yau threefold. In [7] a different method was employed to determine the quantum numbers of the BPS states coming from branes wrapping holomorphic curves in local $\mathbf{P}^2$.

The refined topological vertex formalism solves the problem of finding the all genus partition function for the toric Calabi-Yau threefolds which engineer $U(N_1)\times U(N_2)\times\cdots\times U(N_k)$ theories (including the quivers and matter multiplets in different representations) [7]. The Calabi-Yau geometry is divided in $\mathbb{C}^3$ patches and the partition function is computed by suitably gluing the patches. The refined topological vertex is a function of two parameters $(q,t) := (e^{i\epsilon_1}, e^{-i\epsilon_2})$, labelled by three Young diagrams and it has the following form [7] (see Appendix B for notation and conventions being used):

$$C_{\lambda\,\mu\,\nu}(t,q)=\Big(\frac{q}{t}\Big)^{\frac{\|\mu\|^2}{2}}\,t^{\frac{\kappa(\mu)}{2}}\,q^{\frac{\|\nu\|^2}{2}}\,\widetilde{Z}_\nu(t,q)\sum_{\eta}\Big(\frac{q}{t}\Big)^{\frac{|\eta|+|\lambda|-|\mu|}{2}}\,s_{\lambda^t/\eta}(t^{-\rho}\,q^{-\nu})\,s_{\mu/\eta}(t^{-\nu^t}\,q^{-\rho}), \tag{2.9}$$

where $s_{\lambda/\eta}(\mathbf{x})$ is the skew-Schur function and $\widetilde{Z}_\nu(t,q)$ is given by

$$\widetilde{Z}_\nu(t,q)=\prod_{(i,j)\in\nu}\Big(1-q^{a(i,j)}\,t^{\ell(i,j)+1}\Big)^{-1}.$$

The function $C_{\lambda\,\mu\,\nu}(t,q)\times M(t,q)$, where $M(t,q)=\prod_{i,j=1}^{\infty}(1-q^i\,t^{j-1})^{-1}$ is a refinement of the MacMahon function, is a combinatorial object just like the usual topological vertex [18]. $C_{\lambda\,\mu\,\nu}(t,q)\times M(t,q)$ is the generating function of 3D partitions counting the partitions in an anisotropic way[7]:

$$C_{\lambda\,\mu\,\nu}(t,q)\times M(t,q)=\sum_{\pi(\lambda\,\mu\,\nu)}q^{|\pi(\lambda\,\mu\,\nu)|_\nu}\,t^{|\pi(\lambda\,\mu\,\nu)|-|\pi(\lambda\,\mu\,\nu)|_\nu}, \tag{2.10}$$

where $\pi(\lambda\,\mu\,\nu)$ is 3D partition with asymptotics determined by λ,μ and ν along the three directions and $|\pi(\lambda\,\mu\,\nu)|$ is the regularized total number of boxes in $\pi(\lambda\,\mu\,\nu)$ [18]. The shape of the partition ν along the z-axis determines a slicing of the 3D partition by planes parallel to the z-axis. For the usual vertex this slicing of the 3D partition is just a convenient way of being able to calculate the generating function and the result at the end is independent of this slicing. For the refined vertex case, however, this is not the case and the direction along which we slice breaks the cyclic symmetry of the vertex. This direction along which we slice we will call the preferred direction. Some slices are labelled by q and some slices are labelled by t depending on the shape of the partition ν. $|\pi(\lambda\,\mu\,\nu)|_\nu$ is the number of boxes that fall on the q-slices. Each slice is assigned one of the two counting parameters q or t depending on whether this particular slice is located between an inner,$\{v_i\}$, and outer corner ,$\{u_i\}$, or between an outer and an inner while we trace the profile of ν, Fig. 1.

If all representations labelling the vertex are trivial, the counting is depicted in Fig. 2, and the refined MacMahon function is the generating function of 3D partition with respect to this counting.

For a any partition ν (along the z-axis), it is clear that slices in the x and y direction(far enough) are counted with either q alone or counted with t alone. Thus we see that the two un-preferred directions are either associated with t or with q, *i.e.*, with ϵ_1 or ϵ_2.

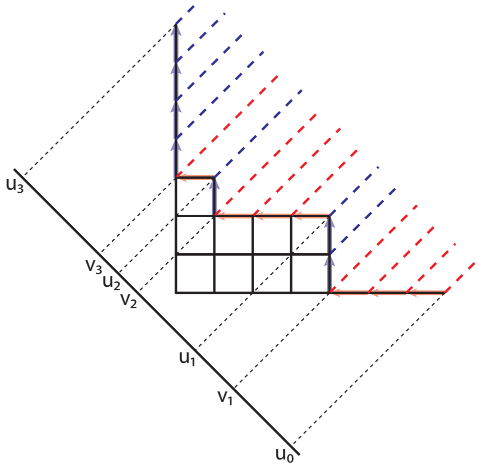

Figure 1. The counting scheme is uniquely determined by the representation along the preferred direction.

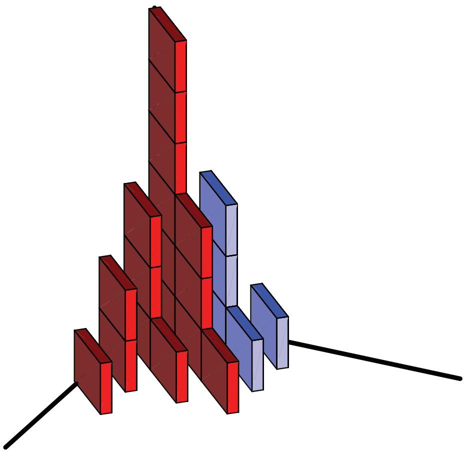

Figure 2. Red slices (left) are counted with t and the blue slices (right) with q.

The A-model topological string theory on a Calabi-Yau threefold X is shown to be the same as the M-theory partition function on [19]

$$X \times S^1 \times TN, \tag{2.11}$$

where TN is the Taub-NUT space. The lift to M-theory provides a novel way to understand the topological A-branes. The A-branes are the M5 branes which wrap the half dimensional Lagrangian submanifolds L in the internal space X and extend in $\mathbb{C} \times S^1 \subset TN \times S^1$. The Taub-NUT space has two cigar subspaces, in the usual topological string theory they can not be distinguished. However, for generic values of $\epsilon_{1,2}$ we have two different of branes [12, 13]. The different type of branes are related to the choice of which un-preferred direction we wrap the A-branes. In other words, the open topological string amplitudes for a stack of A-branes on different un-preferred directions are not the same, unlike in the unrefined topological strings.

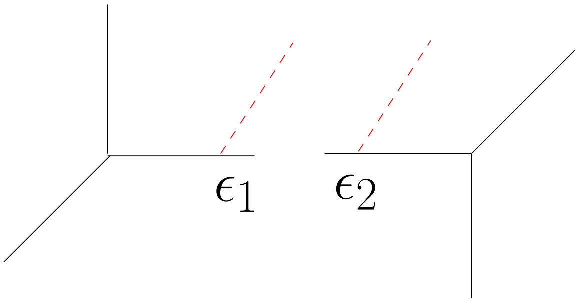

Figure 3. Gluing of two refined vertices

When gluing two refined vertices together along an un-preferred direction we must have the edge of one vertex associated with ϵ_1 and the edge of the second vertex associated with ϵ_2, as shown in Fig. 3 the symmetry between q and t in the refined partition function, which should hold on general grounds Eq.(2.8), is lost.

Also since at each vertex we have a preferred edge, along which we slice in order to define the refined vertex, in the web diagram we will have a number of preferred edges (one for each vertex). Unless all these preferred edges are parallel to each other, i.e., we are slicing all the 3D partitions that appear at the vertices in the same way, the different vertices can not be glued correctly. Hence, a very important constraint of the refined vertex is that all preferred edges in the web diagram should be parallel. As we will discuss in the next section this condition can not always be satisfied and, therefore, refined vertex formalism only works for a certain class of geometries. A web diagram will have set of parallel preferred edges if the corresponding Calabi-Yau threefold is a A_n fibration over a $\mathbf{P}^1$ or a chain of $\mathbf{P}^1$'s.

3 The case of local $\mathbf{P}^2$

In order to calculate the refined partition function of this geometry we need choose at every vertex of the web diagram an edge which is associated with the direction we used to slice the 3D partition. This choice is arbitrary for a given vertex, however, all such edges in the web diagram need to be parallel to each other. This essentially means that we need a set of edges of the web diagram such that this set covers all the vertices and all edges in this set are parallel. It is easy to see that many web diagram fail to have such a set of edges and therefore refined vertex formalism can not be directly applied to such web diagrams.

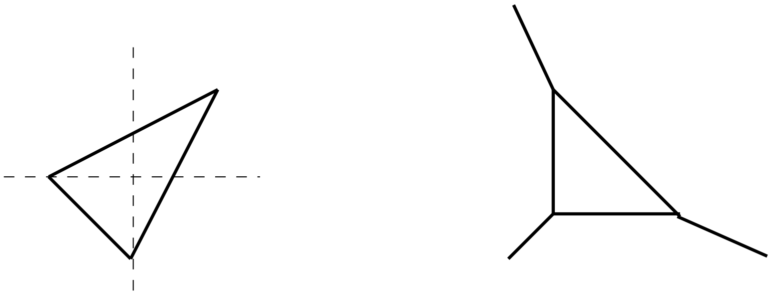

Figure 4. The Newton polygon and the web diagram of local $\mathbf{P}^2$

The simplest geometry which can not be dealt with using the refined topological vertex is $\mathcal{O}(-3) \mapsto \mathbf{P}^2$ also referred to as local $\mathbf{P}^2$. The Newton polygon and the web diagram of this geometry is given in Fig. 4 below.

Recall from the discussion in the last section that the refined vertex is the open string amplitude for branes (along the un-preferred direction) which fill the z_1-plane and the z_2-plane *i.e.*, the two branes on the two un-preferred legs of the vertex are of different kind, one of them is ϵ_1-brane and the other is the ϵ_2-brane. If we choose one of the internal line of the web diagram of local $\mathbf{P}^2$ to be the preferred edge (as shown in Fig. 5) then the refined vertex factor associated with this edge is given by

$$C_{\lambda^t \emptyset \nu}(t,q)\, C_{\emptyset \mu \nu^t}(q,t) \sim \widetilde{Z}_{\nu}(t,q)\widetilde{Z}_{\nu^t}(q,t) \left[s_{\lambda}(t^{-\rho}q^{-\nu})\, s_{\mu}(t^{-\rho}q^{-\nu})\right] \tag{3.1}$$

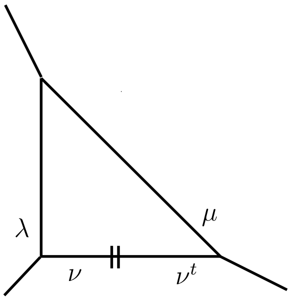

Figure 5. The refined topological vertices can not be consistently glued with the respect to the rules of refined vertex.

It follows from the factor in the square bracket in Eq. (3.1) that the brane on the left lower vertex associated with partition λ and the brane associated with partition μ on the right lower vertex are both ϵ_2-brane. Therefore this suggests that the slicing of the local $\mathbf{P}^2$ web diagram by ϵ_α-branes is such that upper vertex in Fig. 5 has ϵ_1-branes on both its internal legs as shown in Fig. 6.

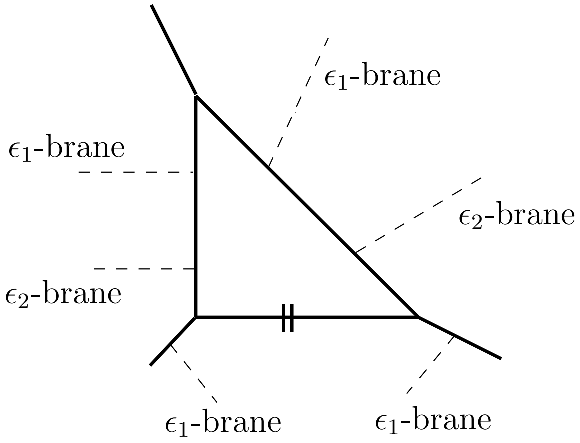

Figure 6. Slicing of the local $\mathbf{P}^2$ web diagram by ϵ_α-branes.

Thus we see that the upper vertex has a different brane configuration then the lower ones which had different ϵ_α branes on there un-preferred edges. Thus we need a new refined topological vertex in which the branes on the un-preferred edges should fill the same plane in the spacetime. Thus to complete the refined vertex formalism and to calculate the refined partition function of local $\mathbf{P}^2$ we need two refined topological vertices corresponding to two different brane configurations as shown in Fig. 7.

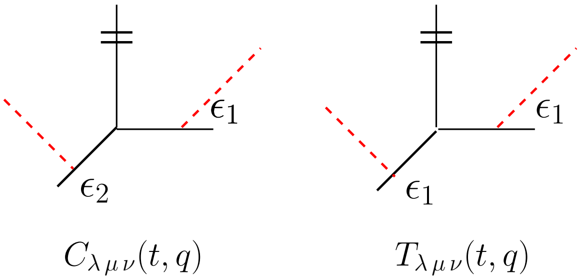

Figure 7. Brane configurations corresponding to two distinct refined vertices. The label $\epsilon_{1,2}$ on the brane indicates which subspace of $\mathbb{C}^2$ it fills.

3.1 The refinement of local $\mathbf{P}^2$

In this section, we will calculate the refined partition function of local $\mathbf{P}^2$ and, along the way, determine the two-legged version of the new refined vertex.

We will begin with local $\mathbf{P}^2$ blown up at one point. The blowup of $\mathbf{P}^2$ is a Hirzebruch surface *i.e.*, it is a $\mathbf{P}^1$ bundle over $\mathbf{P}^1$ such that locally this bundle is $\mathcal{O}(-n)$ over $\mathbf{P}^1$. The local $\mathbf{F}_1$ is then the total space of the canonical bundle on $\mathbf{F}_1$. The Newton polygon and the web diagram of local $\mathbf{F}_1$ is shown in Fig. 8.

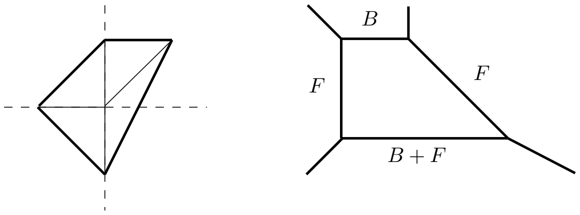

Figure 8. The Newton polygon and the web diagram of local $\mathbf{F}_1$.

B and F are the base and the fiber $\mathbb{P}^1$ respectively and satisfy have the following intersection numbers,

$$B \cdot B = -1\,, \quad F \cdot F = 0\,, \quad B \cdot F = +1\,. \tag{3.2}$$

For a $\mathbf{P}^1$ embedded in a Calabi-Yau threefold the local geometry is $\mathcal{O}(m) \oplus \mathcal{O}(-2-m) \mapsto \mathbf{P}^1$ for some m. In this B is an exceptional curve coming from the blowup of $\mathbf{P}^2$ and has local geometry $\mathcal{O}(-1) \oplus \mathcal{O}(-1) \mapsto B$ i.e., it is resolved conifold. thus the curve B can undergo flop transition which is also clear from the Newton polygon in Fig. 8 which has two distinct triangulations. The flop transition of B can take us from local $\mathbf{F}_1$ to local $\mathbf{P}^2$ as shown in Fig. 9.

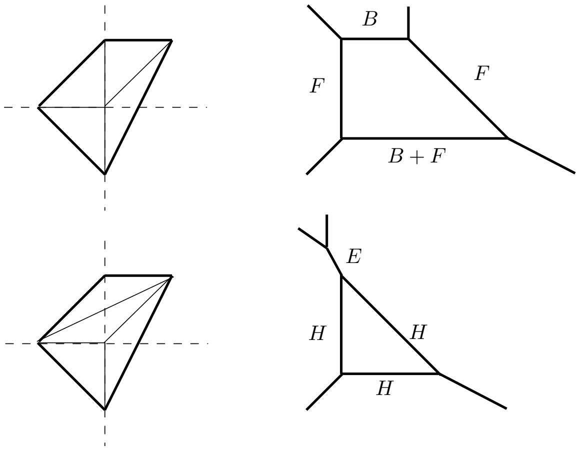

Figure 9. The flop of local $\mathbf{F}_1$ gives rise to local $\mathbf{P}^2$ when the flopped curve is taken to infinite size

The curve E comes from the flop of B and H is the hyperplane class of $\mathbf{P}^2$ and is given by $B + F$. The relation between Kähler parameters on the two sides of the flop is given by

$$Q = Q_b^{-1}\,, \quad Q_H = Q_b Q_f\,, \tag{3.3}$$

where $Q = e^{-t_E}$ is the parameter associated with the curve E.

From Fig. 9 it is clear that we can obtain the refined partition function of local $\mathbf{P}^2$ from the refined partition function of local $\mathbf{F}_1$, $Z_{local\,\mathbf{F}_1}(Q_b, Q_f, t, q)$, if we can follow flop transition in the partition functions:

$$Z_{local\,\mathbf{P}^2}(Q_H, t, q) = \lim_{Q_E \mapsto 0} Z_{local\,\mathbf{F}_1}(Q_E^{-1}, Q_H Q_E, t, q) \tag{3.4}$$

The refined partition function of the local $\mathbf{F}_1$ can be calculated using the refined topological vertex, the two internal horizontal line in the web diagram of the local $\mathbf{F}_1$ (Fig. 8) can serve as the preferred edges, and is given by [7],

$$\begin{aligned} Z_{\mathbf{F}_1}(Q_b, Q_f) :=& \sum_{\nu\,\lambda\,\mu\,\sigma} (-Q_b Q_f)^{|\nu|} (-Q_b)^{|\sigma|} (-Q_f)^{|\lambda|+|\mu|}\, f_\nu^2(q,t)\, \widetilde{f}_\lambda(t,q)\, \widetilde{f}_\mu(q,t) \\ & \times C_{\emptyset\,\lambda\,\nu^t}(t,q)\, C_{\mu^t\,\emptyset\,\nu}(q,t)\, C_{\lambda^t\,\emptyset\,\sigma}(t,q)\, C_{\emptyset\,\mu\,\sigma^t}(q,t), \end{aligned} \tag{3.5}$$

where we are using the following convention for the framing factors[3]

$$f_\lambda(t,q) = (-1)^{|\lambda|}\, t^{\frac{\|\lambda^t\|^2}{2}}\, q^{-\frac{\|\lambda\|^2}{2}}\,, \quad \widetilde{f}_\lambda(t,q) = (-1)^{|\lambda|}\, t^{\frac{\|\lambda^t\|^2 - |\lambda|}{2}}\, q^{-\frac{\|\lambda\|^2 - |\lambda|}{2}}.$$

After the flop transition the relevant variables are $Q = Q_b^{-1}$ and $Q_H = Q_b Q_f$. In terms of these variables the partition function is

$$\begin{aligned} Z_{\mathbf{F}_1}^{flopped}(Q_H, Q) =& \sum_{\nu\,\lambda\,\mu\,\sigma} (-Q_H)^{|\lambda|+|\mu|+|\nu|} (-Q)^{-|\sigma|}\, Q^{|\lambda|+|\mu|}\, f_\nu^2(q,t)\, \widetilde{f}_\lambda(t,q)\, \widetilde{f}_\mu(q,t) \\ & \times C_{\emptyset\,\lambda\,\nu^t}(t,q)\, C_{\mu^t\,\emptyset\,\nu}(q,t)\, C_{\lambda^t\,\emptyset\,\sigma}(t,q)\, C_{\emptyset\,\mu\,\sigma^t}(q,t). \end{aligned} \tag{3.6}$$

Separating the sum involving Q, we can write the partition function as

$$\begin{aligned} Z_{\mathbf{F}_1}^{flopped}(Q_H, Q) =& \sum_{\nu\,\lambda\,\mu\,\sigma} (-Q_H)^{|\lambda|+|\mu|+|\nu|}\, f_\nu^2(q,t)\, \widetilde{f}_\lambda(t,q)\, \widetilde{f}_\mu(q,t)\, C_{\emptyset\,\lambda\,\nu^t}(t,q)\, C_{\mu^t\,\emptyset\,\nu}(q,t) \\ & \times\; Q^{|\lambda|+|\mu|}\, Z_{\lambda\,\mu}(Q^{-1}, t, q), \end{aligned} \tag{3.7}$$

where we have defined

$$Z_{\lambda\,\mu}(Q, t, q) \coloneqq \sum_\sigma (-Q)^{|\sigma|}\, C_{\lambda^t\,\emptyset\,\sigma}(t,q)\, C_{\emptyset\,\mu\,\sigma^t}(q,t). \tag{3.8}$$

In the limit $Q \mapsto 0$, Eq. (16) gives the partition function of the local $\mathbf{P}^2$,

$$Z_{\mathbf{P}^2}(Q_H) = \lim_{Q \mapsto 0} Z_{\mathbf{F}_1}^{flopped}(Q_H, Q)\,. \tag{3.9}$$

---

[3] This convention eliminates the need for shifting certain Kähler parameters by $\frac{\epsilon_1 + \epsilon_2}{2}$.

The Q dependent factor in Eq. (16) can be calculated exactly. We leave the detailed calculation for the next section and here just give the result:

$$\lim_{Q\mapsto 0} Q^{|\lambda|+|\mu|}\, Z_{\lambda\,\mu}(Q^{-1}) = \left(\frac{q}{t}\right)^{\frac{|\lambda|+|\mu|}{2}} (-1)^{|\mu|} f_{\mu^t}(t,q) \sum_{\eta\,\sigma} N^{\eta}_{\lambda\,\mu} U_{\eta\,\sigma}(q,t)\, f_{\sigma}(t,q)\, P_{\sigma}(t^{-\rho};q,t), \tag{3.10}$$

where in the above equation $N^{\eta}_{\lambda\,\mu}$ are the Littlewood-Richardson coefficients, $P_{\sigma}(\mathbf{x};q,t)$ are the Macdonald polynomials and $U_{\eta\,\sigma}(q,t)$ are the transformation matrices which transform Macdonald polynomials to Schur polynomials, $s_{\eta}(\mathbf{x}) = \sum_{\sigma} U_{\eta\,\sigma}(q,t) P_{\sigma}(\mathbf{x};q,t)$.

Thus the refined partition function of locall $\mathbf{P}^2$ is given by

$$\begin{aligned} Z_{local\,\mathbf{P}^2}(Q,t,q) &= \sum_{\lambda\,\mu\,\nu} (-Q)^{|\lambda|+|\mu|+|\nu|}\, q^{\frac{3||\nu^t||^2}{2}}\, t^{-\frac{||\nu||^2}{2}}\, \widetilde{Z}_{\nu}(q,t) \widetilde{Z}_{\nu^t}(t,q) \times \\ & s_{\lambda}(q^{-\rho}t^{-\nu})\, s_{\mu}(q^{-\rho}t^{-\nu}) \left(\frac{q}{t}\right)^{\frac{|\lambda|-|\mu|}{2}} N^{\eta}_{\lambda\,\mu} \Big[\sum_{\sigma} U_{\eta\,\sigma} t^{\frac{||\eta^t||^2}{2}} q^{-\frac{||\eta||^2}{2}}\, P_{\sigma}(t^{-\rho};q,t)\Big]. \end{aligned} \tag{3.11}$$

Define

$$T_{\mu\,\lambda\,\emptyset}(t,q) := (-1)^{|\mu|} \left(\frac{t}{q}\right)^{|\lambda|} f_{\lambda}(q,t)\, f^2_{\mu^t}(t,q) \sum_{\eta\,\sigma} N^{\eta}_{\lambda^t\,\mu} U_{\eta\,\sigma}(q,t)\, f_{\sigma}\, P_{\sigma}(t^{-\rho};q,t)$$

Then from Eq. (3.11) it follows that

$$\begin{aligned} Z_{\mathbf{P}^2}(Q_H) = \sum_{\lambda\,\mu\,\nu} & (-Q_H)^{|\lambda|+|\mu|+|\nu|} \Big(f_{\nu}(q,t)\, \widetilde{f}_{\lambda}(t,q)\, \widetilde{f}_{\mu}(q,t)\Big)^2 \\ & C_{\emptyset\,\lambda\,\nu^t}(t,q) C_{\mu^t\,\emptyset\,\nu}(q,t)\, T_{\mu\,\lambda^t\,\emptyset} \end{aligned} \tag{3.12}$$

We have verified, up to order Q_H^3, that the above partition function gives the correct BPS degeneracies for local $\mathbf{P}^2$. The form of the partition function given above suggests that $T_{\lambda\,\mu\,\emptyset}(t,q)$ is a new two-legged topological vertex which can be used to determine the refined partition function of the local $\mathbf{P}^2$ using the usual gluing rule.

4 The New Refined Vertex

In this section, we derive the new refined vertex by placing the branes on the resolved conifold and then letting the geometry undergo a flop transition. The brane configuration on the resolved conifold that we will begin with corresponds to the Hopf link and was studied in [20]. The relation of this brane configuration and its corresponding amplitude with the refined Chern-Simons theory was discussed in [21].

In the next section we will clarify further the relation between the refined topological vertex, the new vertex and the refined Chern-Simons theory. We will see that the refined topological vertex and the new vertex together capture all the information of the refined Chern-Simons theory.

Let us begin, as is always the case when considering knots in the open topological string theory, with T^*S^3, the cotangent of S^3. Consider the Hopf link embedded in S^3 which is the zero section of T^*S^3. The two unknots which make up the Hopf link are colored by two representations λ and μ. When this setup is embedded in M-theory we consider compactification on $T^*S^3 \times S^1 \times \mathbb{C}^2$ with M5-branes wrapping $L_1 \times S^1 \times C_1$ and $L_2 \times S^1 \times C_2$. $L_{1,2}$ are two Lagrangian cycles with boundary the two unknots of the Hopf link. $C_{1,2}$ are 2 dimensional planes in $\mathbb{C}^2$ given by $z_1 = 0$ and $z_2 = 0$ respectively. In the refined topological string theory, two choices for the branes on Lagrangian cycles: either both M5-branes fill z_1-plane (or z_2-plane) or one brane fills the z_1-plane and the other z_2-plane as shown in Fig. 10. We will denote these two configurations with $\mathcal{C}_1$ and $\mathcal{C}_2$, respectively.

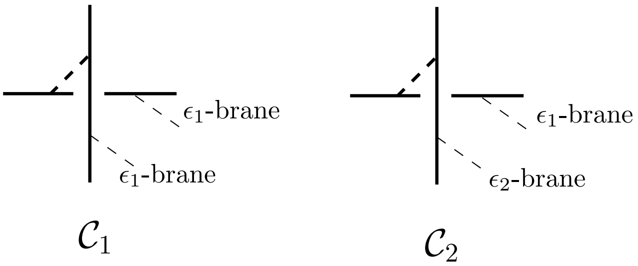

Figure 10. Two distinct brane configurations on T^*S^3.

When the T^*S^3 undergoes geometric transition S^3 shrinks to zero size and is replaced with an S^2. The total space becomes a complex bundle over $\mathbf{P}^1$, $\mathcal{O}(-1) \oplus \mathcal{O}(-1) \mapsto \mathbf{P}^1$. The two configurations $\mathcal{C}_{1,2}$, after the geometric transition, correspond to the two A-brane configurations shown in Fig. 11.

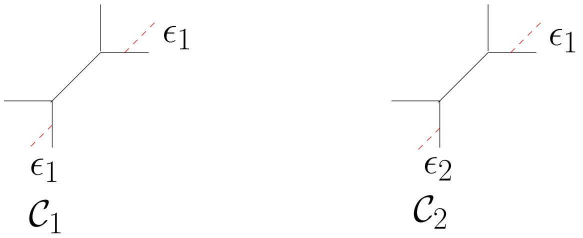

Figure 11. In the refined open topological string theory, the branes are distinguished with respect to which $\mathbb{R}^2 \subset \mathbb{R}^4$ they fill.

The two different configurations of branes given above give two different partition functions. The brane configuration in $\mathcal{C}_1$ is the same brane configuration for the Hopf link studied in [20]. In this brane configuration, the M5-branes wrapping both Lagrangian submanifolds on the different legs of the resolved conifold fill the z_1-plane in $\mathbb{C}^2$. The BPS particles due to M2-branes wrapping the discs ending on M5-branes carry spin under the $U(1)$ rotation of the z_1-plane (they also carry $U(1)$ R-charge which is the $U(1)$ rotation of the orthogonal z_2-plane). The BPS particles correspond to holomorphic functions on the z_1-plane and therefore the open string partition function of this brane configuration will have denominator a function of q only. However, in $\mathcal{C}_2$, the branes are extending in both z_1- and z_2-planes, and depending on which discs M2-branes are wrapping, the BPS particles are charged under both $U(1)$'s and the denominator of the open string partition function in this case will be function of both t and q.

4.1 Derivation of the two-legged new vertex

In this subsection, we will present the derivation of the new vertex. This subsection and the next one include the more technical details. We collect some of the identities used in the derivation in Appendix B.

The configuration $\mathcal{C}_1$ after the flop corresponds to the refined Hopf link [20] and the corresponding open string partition function is given by,

$$Z_{\lambda\,\mu}(Q,t,q)=\sum_{\nu}(-Q)^{|\nu|}\,C_{\lambda^t\,\emptyset\,\nu}(t,q)\,C_{\emptyset\,\mu\,\nu^t}(q,t), \tag{4.1}$$

where $T=-\log(Q)$ is the Kähler parameter of the $\mathbf{P}^1$.

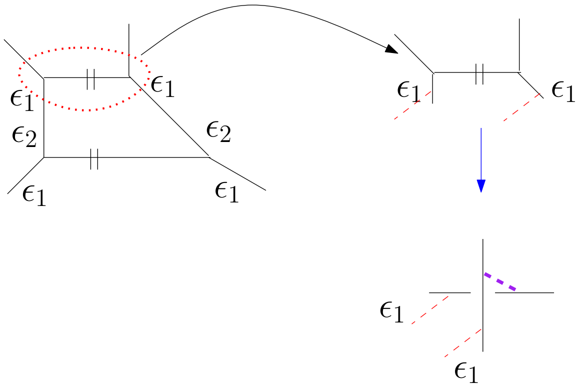

Figure 12. The relation between the Hopf link and the legged version of the new vertex.

As shown in Fig. 12 the configuration $\mathcal{C}_1$ of branes is precisely what appears in the local $\mathbf{F}_1$. Thus if we can follow the flop in the refined Hopf link partition function we can determine the two-legged version of the new vertex which appeared in Eq.(3.12).

After the flop the corresponding partition function will be (up to framing factors), in terms of the new vertex $T_{\lambda\,\mu\,\nu}(t,q)$,

$$Z_{\lambda\,\mu}(Q^{-1},t,q)\sim\sum_{\nu}Q^{-|\nu|}\,T_{\lambda\,\mu\,\nu}(t,q)T_{\emptyset\,\emptyset\,\nu^t}(q,t)\,. \tag{4.2}$$

We will see that the expression for $T_{\lambda\,\mu\,\nu}(t,q)$ can be read from the partition function Eq. (4.1) by analytic continuation Q to Q^{-1} so that

$$Z^{flop}_{\lambda\,\mu}(Q,t,q)\sim Z_{\lambda\,\mu}(Q^{-1},t,q)\,. \tag{4.3}$$

Although $Z_{\lambda\,\mu}(Q,t,q)$ is an infinite series in Q, the normalized open string partition function

$$G_{\lambda\,\mu}(Q):=\frac{Z_{\lambda\,\mu}(Q,t,q)}{Z_{\emptyset\,\emptyset}(Q,t,q)}=\frac{\sum_{\sigma}(-Q)^{|\sigma|}\,C_{\lambda^t\,\emptyset\,\sigma}(t,q)\,C_{\emptyset\,\mu\,\sigma^t}(q,t)}{\sum_{\sigma}(-Q)^{|\sigma|}\,C_{\emptyset\,\emptyset\,\sigma}(t,q)\,C_{\emptyset\,\emptyset\,\sigma^t}(q,t)} \tag{4.4}$$

is a polynomial of degree $|\lambda|+|\mu|$ in Q. This was conjectured in [20] and proven in [22]. Notice that $Z_{\emptyset\,\emptyset}(Q)$ is the closed string partition function of the geometry $\mathcal{O}_{\mathbb{P}^1}(-1)\oplus\mathcal{O}_{\mathbb{P}^1}(-1)$ and is invariant under the flop,[4]

$$Z_{\emptyset\,\emptyset}(Q^{-1},t,q)=Z_{\emptyset\,\emptyset}(Q,t,q)\,. \tag{4.5}$$

Thus we can obtain the expression for the flopped partition function by studying $G_{\lambda\,\mu}(Q,t,q)$. Using the definition of the refined topological vertex we can write $G_{\lambda\,\mu}(Q,t,q)$ as

$$G_{\lambda\,\mu}(Q)=(-1)^{|\mu|}\left(\frac{q}{t}\right)^{\frac{|\lambda|+|\mu|}{2}}f_{\mu^t}\frac{\sum_{\nu}(-Q)^{|\nu|}\,q^{\frac{\|\nu\|^2}{2}}\,t^{\frac{\|\nu^t\|^2}{2}}\,\widetilde{Z}_{\nu}(t,q)\,\widetilde{Z}_{\nu^t}(q,t)\,s_{\lambda}(t^{-\rho}q^{-\nu})\,s_{\mu}(t^{-\rho}q^{-\nu})}{\sum_{\nu}(-Q)^{|\nu|}\,q^{\frac{\|\nu\|^2}{2}}\,t^{\frac{\|\nu^t\|^2}{2}}\,\widetilde{Z}_{\nu}(t,q)\,\widetilde{Z}_{\nu^t}(q,t)}\,.$$

Since the two Schur functions in the summation above have the same argument we can use

$$s_{\lambda}(\mathbf{x})\,s_{\mu}(\mathbf{x})=\sum_{\eta}N^{\eta}_{\lambda\,\mu}s_{\eta}(\mathbf{x}), \tag{4.6}$$

to write the normalized open amplitude as

$$G_{\lambda\,\mu}(Q,t,q)=(-1)^{|\mu|}\left(\frac{q}{t}\right)^{\frac{|\lambda|+|\mu|}{2}}f_{\mu^t}(t,q)\frac{1}{Z_{\emptyset\,\emptyset}}\sum_{\eta}N^{\eta}_{\lambda\,\mu}\,H_{\eta}(Q,t,q) \tag{4.7}$$

$$H_{\eta}(Q,t,q):=\sum_{\nu}(-Q)^{|\nu|}\,q^{\frac{\|\nu\|^2}{2}}\,t^{\frac{\|\nu^t\|^2}{2}}\,\widetilde{Z}_{\nu}(t,q)\,\widetilde{Z}_{\nu^t}(q,t)\,s_{\eta}(t^{-\rho}q^{-\nu}).$$

---

[4] It is invariant if we ignore the shift in the classical contribution which arises due to the flop.

Following [22], we express the Schur function in terms of Macdonald function to obtain

$$
\begin{aligned}
H_{\eta}(Q,t,q) &= \sum_{\sigma} U_{\eta\,\sigma}(q,t) J_{\sigma}(Q,t,q) \\
J_{\sigma}(Q,t,q) &:= \sum_{\nu} (-Q)^{|\nu|}\, q^{\frac{\|\nu\|^2}{2}}\, t^{\frac{\|\nu^t\|^2}{2}}\, \widetilde{Z}_{\nu}(t,q)\, \widetilde{Z}_{\nu^t}(q,t)\, P_{\sigma}(t^{-\rho}q^{-\nu};q,t),
\end{aligned}
\tag{4.8}
$$

where the $U_{\eta\,\sigma}(q,t)$ are the previously defined matrices which take Macdonald functions to Schur functions. $s_{\eta}(\mathbf{x})$ and $P_{\sigma}(\mathbf{x};q,t)$ are both homogenous functions of degree of $|\eta|$ and $|\sigma|$, respectively, hence, $U_{\eta\,\sigma}(q,t)=0$ if $|\eta|\neq|\sigma|$. Also it follows from the definition of the Macdonald function that $U_{\eta\,\sigma}=\delta_{\eta\,\sigma}$ for $t=q$.

The normalized Hopf link partition function in terms of J_{σ} is given by

$$
G_{\lambda\,\mu}(Q) = (-1)^{|\mu|}\left(\frac{q}{t}\right)^{\frac{|\lambda|+|\mu|}{2}} f_{\mu^t}(t,q)\frac{1}{Z_{\emptyset\,\emptyset}(Q)}\sum_{\eta\;\sigma} N_{\lambda\,\mu}^{\eta}\, U_{\eta\,\sigma}(q,t)\, J_{\sigma}(Q,t,q). \tag{4.9}
$$

The principal specialization of the Macdonald polynomials are proportional to $\widetilde{Z}_{\nu}(t,q)$

$$
t^{\frac{\|\nu^t\|^2}{2}}\, \widetilde{Z}_{\nu}(t,q) = P_{\nu}(t^{-\rho};q,t), \tag{4.10}
$$

$J_{\sigma}(Q,t,q)$ can be written in terms of Macdonald functions

$$
J_{\sigma}(Q,t,q) = \sum_{\nu} (-Q)^{|\nu|}\; P_{\nu^t}(q^{-\rho};t,q)\, P_{\nu}(t^{-\rho};q,t)\, P_{\sigma}(t^{-\rho}q^{-\nu};q,t). \tag{4.11}
$$

The sum of the partition ν can be performed by making use of the identity ([23], Page 332, Eq.(6.6))

$$
P_{\nu}(t^{-\rho};q,t)P_{\sigma}(q^{-\nu}\,t^{-\rho};q,t) = P_{\sigma}(t^{-\rho};q,t)\, P_{\nu}(q^{-\sigma}\,t^{-\rho};q,t), \tag{4.12}
$$

$J_{\sigma}(Q,t,q)$ takes a product form

$$
\begin{aligned}
J_{\sigma}(Q,t,q) &= \sum_{\nu} (-Q)^{|\nu|}\, P_{\nu^t}(q^{-\rho};t,q)\, P_{\sigma}(t^{-\rho};q,t)\, P_{\nu}(t^{-\rho}q^{-\sigma};q,t) \\
&= P_{\sigma}(t^{-\rho};q,t)\sum_{\nu} (-Q)^{|\nu|}\, P_{\nu^t}(q^{-\rho};t,q)\, P_{\nu}(t^{-\rho}q^{-\sigma};q,t) \\
&= P_{\sigma}(t^{-\rho};q,t)\,\prod_{i,j=1}^{\infty}\left(1 - Q\,t^{-\rho_i}\,q^{-\rho_j-\sigma_i}\right),
\end{aligned}
\tag{4.13}
$$

where we have used the identity [23]

$$\sum_{\nu} P_{\nu}(\mathbf{x};q,t)\, P_{\nu^t}(\mathbf{y};t,q) = \prod_{i,j=1}^{\infty} (1+x_i\, y_j)\,. \tag{4.14}$$

We can factorize the infinite product as a finite product over the boxes of a Young diagram and an infinite one to normalize $J_{\sigma}(Q,t,q)$:

$$J_{\sigma}(Q,t,q) = \left[P_{\sigma}(t^{-\rho};q,t) \prod_{(i,j)\in\sigma} (1-Q\, t^{i-\frac{1}{2}}\, q^{-j+\frac{1}{2}}) \right] \times \prod_{i,j=1}^{\infty} \left(1-Q\, t^{i-\frac{1}{2}}\, q^{j-\frac{1}{2}}\right) \tag{4.15}$$

$$\frac{J_{\sigma}(Q,t,q)}{J_{\emptyset}(Q,t,q)} = P_{\sigma}(t^{-\rho};q,t) \prod_{(i,j)\in\sigma} (1-Q\, t^{i-\frac{1}{2}}\, q^{-j+\frac{1}{2}}).$$

$J_{\emptyset}(Q,t,q) = Z_{\emptyset\,\emptyset}(Q,t,q)$ is the closed string partition function for the resolved conifold. Thus the normalized refined Hopf link partition function can be written as[5]

$$G_{\lambda\,\mu}(Q) = (-1)^{|\mu|} \left(\frac{q}{t}\right)^{\frac{|\lambda|+|\mu|}{2}} f_{\mu^t}(t,q) \sum_{\eta\;\sigma} N^{\eta}_{\lambda\,\mu} U_{\eta\,\sigma}(q,t)\, P_{\sigma}(t^{-\rho};q,t) \prod_{(i,j)\in\sigma} (1-Q\, t^{i-\frac{1}{2}}\, q^{-j+\frac{1}{2}}). \tag{4.17}$$

Before we continue with the derivation of the new vertex, let us argue that the normalized partition function for the Hopf link is a polynomial in Q of order $|\lambda|+|\mu|$. We know that $N^{\eta}_{\lambda\,\mu}$ is zero unless $|\lambda|+|\mu| = |\eta|$ and $U_{\eta\,\sigma}(t,q)$ vanishes for $|\eta| \neq |\sigma|$. Therefore, we conclude that the sum is finite, and the product is of finite order. $G_{\lambda\,\mu}(Q,t,q)$ is of the order $|\lambda|+|\mu|$.

The two legged new vertex will be obtained by taking the flop transition and sending the Kähler parameter to infinity. Let us define $Q_{\bullet} = Q^{-1}$ to take the limit

---

[5] The normalized Hopf link partition function can be even written in a more compact way realizing that

$$P_{\sigma}(t^{-\rho}, z\, t^{\rho};q,t) = P_{\sigma}(t^{-\rho};q,t) \prod_{(i,j)\in\sigma} (1-z\, q^{j-1}\, t^{-i+1}). \tag{4.16}$$

$G_{\lambda\,\mu}(Q,t,q)$ takes then the following form

$$G_{\lambda\,\mu}(Q) = (-1)^{|\mu|} \left(Q\sqrt{\frac{q}{t}}\right)^{|\lambda|+|\mu|} f_{\mu^t}(t,q) \sum_{\eta\;\sigma} N^{\eta}_{\lambda\,\mu} U_{\eta\,\sigma}(q,t)\, f_{\sigma}(t,q)\, P_{\sigma}\left(t^{-\rho}, Q^{-1}\sqrt{\frac{q}{t}}\, t^{\rho};q,t\right).$$

after the flop transition, we can write

$$\prod_{(i,j)\in\sigma}\Big(1-Q\,t^{i-\frac{1}{2}}\,q^{-j+\frac{1}{2}}\Big) = \prod_{(i,j)\in\sigma}\Big(1-Q_{\bullet}^{-1}\,t^{i-\frac{1}{2}}\,q^{-j+\frac{1}{2}}\Big) \tag{4.18}$$
$$= (-Q_{\bullet})^{-|\sigma|}\,t^{\frac{\|\sigma^t\|^2}{2}}\,q^{-\frac{\|\sigma\|^2}{2}}\prod_{(i,j)\in\sigma}\Big(1-Q_{\bullet}\,t^{-i+\frac{1}{2}}\,q^{j-\frac{1}{2}}\Big)$$

The limit to define the two-legged vertex (up to framing and overall factors) can be easily taken using the following form of the normalized Hopf link partition function

$$G_{\lambda\,\mu}(Q) = (-1)^{|\mu|}\left(-Q\sqrt{\frac{t}{q}}\right)^{|\lambda|+|\mu|} f_{\mu^t}(t,q)\sum_{\eta\,\sigma} N_{\lambda\,\mu}^{\eta}U_{\eta\,\sigma}(q,t)\,t^{\frac{||\sigma^t||^2}{2}}\,q^{-\frac{||\sigma||^2}{2}}\,P_{\sigma}(t^{-\rho};q,t)$$
$$\times\prod_{(i,j)\in\sigma}\Big(1-Q^{-1}\,t^{-i+\frac{1}{2}}\,q^{j-\frac{1}{2}}\Big). \tag{4.19}$$

From the above equation we see that

$$T_{\mu\,\lambda^t\,\emptyset}(t,q) \propto \lim_{Q\mapsto 0} Q^{|\lambda|+|\mu|}\,Z_{\lambda\,\mu}(Q^{-1}) = \lim_{Q\mapsto 0} Q^{|\lambda|+|\mu|}\,Z_{\emptyset\,\emptyset}(Q^{-1})\,G_{\lambda\,\mu}(Q^{-1}) \tag{4.20}$$
$$= (-1)^{|\mu|}\left(\frac{t}{q}\right)^{\frac{|\lambda|}{2}} f_{\mu^t}(t,q)\sum_{\eta\,\sigma} N_{\lambda\,\mu}^{\eta}U_{\eta\,\sigma}(q,t)\,f_{\sigma}(t,q)\,P_{\sigma}(t^{-\rho};q,t).$$

Notice that we have made use of the invariance of the resolved conifold partition function under flop, $Z_{\emptyset\,\emptyset}(Q^{-1},t,q) = Z_{\emptyset\,\emptyset}(Q,t,q)$

4.2 The new vertex

In this subsection, we will derive a three-legged new topological vertex from the flop of the refined Hopf link invariant. Together with the refined topological vertex this new vertex will complete the refined vertex formalism which can then be used for any non-compact toric Calabi-Yau threefold.

From the results of the previous section (Eq. 4.19), we have

$$G_{\lambda\,\mu}(Q) = (-1)^{|\mu|}\left(Q\sqrt{\frac{q}{t}}\right)^{|\lambda|+|\mu|} f_{\mu^t}(t,q)\sum_{\eta\,\sigma} N_{\lambda\,\mu}^{\eta}U_{\eta\,\sigma}(q,t)\,f_{\sigma}(t,q)\,P_{\sigma}(t^{-\rho};q,t)$$
$$\times\prod_{(i,j)\in\sigma}\Big(1-Q^{-1}\,t^{-i+\frac{1}{2}}\,q^{j-\frac{1}{2}}\Big)$$

Now that we have a polynomial expression for $G_{\lambda\,\mu}$ we can determine the flopped vertex.

$$\begin{aligned} Z_{\emptyset\,\emptyset}(Q^{-1}) \prod_{(i,j)\in\sigma} \left(1 - Q^{-1}\, t^{-i+\frac{1}{2}}\, q^{j-\frac{1}{2}}\right) &= \prod_{i,j=1}^{\infty} \left(1 - Q^{-1}\, t^{i-\frac{1}{2}}\, q^{j-\frac{1}{2}}\right) \prod_{(i,j)\in\sigma} \left(1 - Q^{-1}\, t^{-i+\frac{1}{2}}\, q^{j-\frac{1}{2}}\right) \\ &= \sum_{\nu} (-Q)^{-|\nu|} P_{\nu^t}(q^{\rho}; t, q)\, P_{\nu}(t^{\rho}\, q^{\sigma}; q, t) \end{aligned}$$

Using the identity

$$P_{\nu}(t^{\rho} q^{\sigma}; q, t) = \frac{P_{\sigma}(t^{\rho} q^{\nu}; q, t)\, P_{\nu}(t^{\rho}; q, t)}{P_{\sigma}(t^{\rho}; q, t)} \tag{4.21}$$

we get

$$\begin{aligned} Z_{\lambda\,\mu}(Q) &= (-1)^{|\mu|} \left(Q\sqrt{\frac{q}{t}}\right)^{|\lambda|+|\mu|} f_{\mu^t}(t, q) \sum_{\nu\,\eta\,\sigma} (-Q)^{-|\nu|}\, N_{\lambda\,\mu}^{\eta}\, U_{\eta\,\sigma}(q, t)\, f_{\sigma}(t, q)\, P_{\nu^t}(q^{\rho}; t, q) \\ &\quad \times \left(\frac{P_{\sigma}(t^{-\rho}; q, t)}{P_{\sigma}(t^{\rho}; q, t)}\right) P_{\nu}(t^{\rho}; q, t)\, P_{\sigma}(t^{\rho} q^{\nu}; q, t). \end{aligned}$$

The ratio in the parentheses can be simplified to a factor proportional to the framing factor

$$\frac{P_{\sigma}(t^{-\rho}; q, t)}{P_{\sigma}(t^{\rho}; q, t)} = (-1)^{|\sigma|}\, t^{\frac{\|\sigma^t\|^2}{2}}\, q^{-\frac{\|\sigma\|^2}{2}} \left(\frac{q}{t}\right)^{\frac{|\sigma|}{2}} = \left(\frac{q}{t}\right)^{\frac{|\sigma|}{2}} f_{\sigma}(t, q). \tag{4.22}$$

Notice that

$$\begin{aligned} Z_{\lambda\,\mu}(Q) &= (-1)^{|\mu|} \left(Q\frac{q}{t}\right)^{|\lambda|+|\mu|} f_{\mu^t}(t, q) \sum_{\nu\,\eta\,\sigma} (-Q)^{-|\nu|}\, N_{\lambda\,\mu}^{\eta}\, U_{\eta\,\sigma}(t, q)\, f_{\sigma}^2(t, q)\, P_{\nu^t}(q^{\rho}; t, q) \\ &\quad \times P_{\nu}(t^{\rho}; q, t)\, P_{\sigma}(t^{\rho} q^{\nu}; q, t) \end{aligned}$$

Isolating the ν sum, the preferred direction, we define $\widetilde{C}_{\lambda\,\mu\,\nu}(t, q)$

$$\begin{aligned} Q^{|\lambda|+|\mu|}\, G_{\lambda\,\mu}(Q^{-1}) &= \sum_{\nu} (-Q)^{|\nu|} P_{\nu^t}(q^{\rho}; t, q)\, \widetilde{C}_{\lambda\,\mu\,\nu}(t, q) \\ \widetilde{C}_{\lambda\,\mu\,\nu}(t, q) &= (-1)^{|\mu|}\, f_{\mu^t}(t, q)\, P_{\nu}(t^{\rho}; q, t) \sum_{\eta\,\sigma} N_{\lambda\,\mu}^{\eta}\, U_{\eta\,\sigma}(t, q)\, f_{\sigma}^2(t, q)\, P_{\sigma}(t^{\rho} q^{\nu}; q, t) \end{aligned} \tag{4.23}$$

Define the new topological vertex as

$$T_{\lambda\,\mu\,\nu}(t, q) := \left(\sqrt{\frac{t}{q}}\right)^{|\mu|-|\lambda|} \frac{1}{f_{\lambda^t}(t, q)\, f_{\mu}(q, t)}\, \widetilde{C}_{\lambda^t\,\mu\,\nu}(t, q)$$

After some simplification the new topological vertex can be written as

$$\begin{aligned} T_{\lambda\,\mu\,\nu} = &\left(\sqrt{\frac{t}{q}}\right)^{|\mu|-|\lambda|}(-1)^{|\mu|}\, f^2_{\mu^t}(t,q)\, f_\lambda(q,t)\, P_\nu(t^\rho;q,t) \\ &\sum_{\eta\,\sigma} N^{\eta}_{\lambda^t\,\mu}\, U_{\eta\,\sigma}\, f^2_\sigma\, P_\sigma(t^\rho q^\nu;q,t) \end{aligned} \tag{4.24}$$

5 Gluing Rules for the New Vertex with the Refined Topological Vertex

In this section, we will describe the algorithm that will allow us to compute the refined topological string partition function for any given toric Calabi-Yau threefold. As argued in [24], any toric Calabi-Yau threefold can be obtained from a large enough fiducial geometry by a series of flop transitions and sending some of the unwanted Kähler moduli to infinity. The fiducial geometry that we will use is a ladder diagram, such as the one depicted in the right upper corner in Fig. 14. Each vertex in this diagram locally corresponds to T^*S^3 where the S^3 has shrunk.

Consider T^*S^3 with N M5-branes wrapped on S^3 and extending in the z_2-plane along with two stacks of M5-branes on the wrapped on Lagrangian cycles $\mathcal{L}_1$ and $\mathcal{L}_2$, which have the topology of $S^1 \times \mathbb{R}^2$, and extending in the z_2-plane. The Lagrangian cycles are shown as dotted line in Fig. 18. In going through the large N transition the singular geometry, when the S^3 has shrunk, can resolve itself in two different ways related to each other by a flop as shown in Fig. 18.

The rules are pretty simple:

- Start with the ladder diagram and resolve each node
- Associate the preferred direction of the refined topological vertex every time a node is resolved by $N \mapsto -\infty$
- Associate the preferred direction of the new topological vertex every time a node is resolved by $N \mapsto \infty$
- The assignment of the preferred direction remains unchanged if the flopped edge is not along one of preferred directions

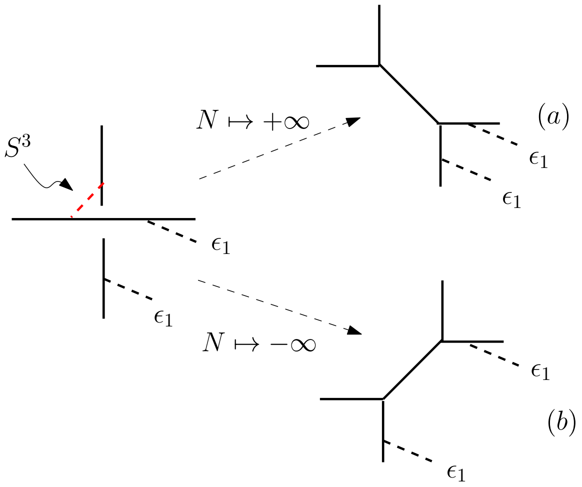

Figure 13. The large N transition can resolve the conifold in two different ways.

- Flopping an edge along the preferred direction changes the time of the vertex, *i.e.*, if the preferred direction of the refined topological vertex is flopped it become the preferred direction of the new topological vertex, vice versa.
- Assignment of the propagators and $t, q-$identifications are the same as the refined topological vertex

After these rules are applied, it is easy to see that the different type of preferred directions remain parallel among each other. An example with different choices of flops is depicted in Fig. 14.

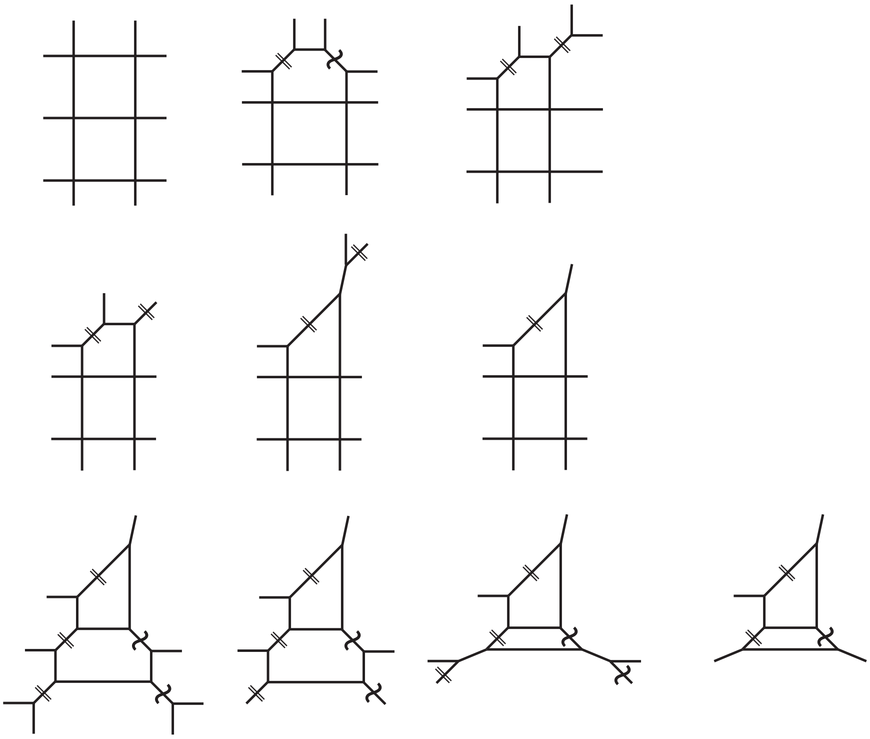

Figure 14. Different choice of resolutions of the nodes in the ladder diagram and the associated assignments of the preferred directions.

6 Applications of the new vertex

In this section, we want to work out some examples using the new topological vertex.

6.1 Example 1: $\mathcal{O}_{\mathbf{P}^1}(-1) \oplus \mathcal{O}_{\mathbf{P}^1}(-1)$

The first geometry we want to consider is the resolved conifold. Similar to the refined topological vertex computation we can perform the computation in different ways depending on our choice of gluing the vertices. Our first gluing is in the following way

$$\begin{aligned} Z &= \sum_{\nu} (-Q)^{|\nu|}\, T_{\emptyset\,\emptyset\,\nu}(t,q)\, T_{\emptyset\,\emptyset\,\nu^t}(q,t) \\ &= \sum_{\nu} (-Q)^{|\nu|}\, P_{\nu}(t^{\rho}; q,t)\, P_{\nu^t}(q^{\rho}; t,q) = \prod_{i,j=1}^{\infty} \left(1 - Q\, q^{i-\frac{1}{2}}\, t^{j-\frac{1}{2}}\right) \end{aligned} \tag{6.1}$$

which agrees with the refined topological string partition function in [7]. The second way of gluing the new vertices gives the same refined partition function:

$$
\begin{aligned}
Z &= \sum_{\lambda}(-Q)^{|\lambda|}\,T_{\lambda\,\emptyset\,\emptyset}(t,q)\,T_{\lambda^t\,\emptyset\,\emptyset}(q,t) \qquad (6.2)\\
&= \sum_{\sigma_1\,\sigma_2}(-Q)^{|\sigma_1|}\,f^2_{\sigma_1}(t,q)\,f^2_{\sigma_2}(q,t)\,P_{\sigma_1}(t^\rho;q,t)\,P_{\sigma_2}(q^\rho;t,q)\sum_{\lambda}U_{\lambda^t\,\sigma_1}(t,q)\,U_{\lambda\,\sigma_2}(q,t)\\
&= \sum_{\sigma_1}(-Q)^{|\sigma_1|}\,P_{\sigma_1}(t^\rho;q,t)P_{\sigma_1^t}(q^\rho;t,q) = \prod_{i,j}\left(1-Q\,q^{i-\frac{1}{2}}\,t^{j-\frac{1}{2}}\right)
\end{aligned}
$$

where in simplifying the second line we have used

$$
f_\eta(t,q)\,f_{\eta^t}(q,t)=1\,,\qquad U^T(t,q)\,J\,U(q,t)=J \quad \text{where} \quad (J)_{\sigma\,\eta}=\delta_{\sigma\,\eta^t} \qquad (6.3)
$$

6.2 Example 2: Local $\mathbf{P}^1\times\mathbf{P}^1$

The topological string partition of local $\mathbf{P}^1\times\mathbf{P}^1$ can be computed using the refined topological vertex [7]. Using the new topological vertex we can re-calculate its partition function but with the different choice of the preferred direction which was not allowed according to the gluing rules of the refined topological vertex. Fig. 15 demonstrates the basic idea and the choice of gluing.

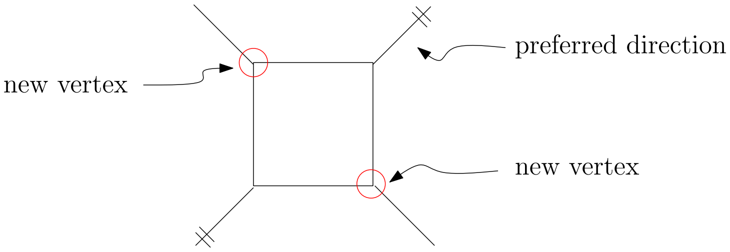

Figure 15. The computation of the partition function of local $\mathbf{P}^1\times\mathbf{P}^1$ using the new topological vertex. Circled vertices are the ones where the new vertex is used.

From our previous discussion of the new topological vertex we can rewrite this expression as

$$
\begin{aligned}
Z = \sum_{\lambda\,\mu\,\delta\,\sigma}(-Q_b)^{|\lambda|+|\delta|}(-Q_f)^{|\mu|+|\sigma|}\quad & \widetilde{f}_\lambda(t,q)\widetilde{f}_\mu(t,q)\widetilde{f}_\sigma(q,t)\widetilde{f}_\delta(q,t)\,C_{\lambda\,\mu^t\,\emptyset}(q,t)\,C_{\delta\,\sigma^t\,\emptyset}(t,q)\\
&\times T_{\sigma\,\lambda^t\,\emptyset}(t,q)\,T_{\mu\,\delta^t\,\emptyset}(q,t)
\end{aligned}
$$

6.3 Example 3: Local $\mathbf{F}_1$

The local $\mathbf{F}_1$ refined partition was calculated in section 3 for a particular choice of the preferred direction. Here we use the new vertex to calculate it using a different

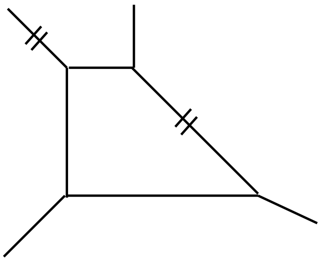

Figure 16. The choice of preferred edges for local $\mathbf{F}_1$.

preferred direction. The web diagram of local $\mathbf{F}_1$ and the choice of the preferred direction is shown in Fig. 16.

The partition function can be calculated easily using the rules discussed in the last section and is given by

$$Z(Q_b,Q_f) = \sum_{\lambda\,\mu\,\tau\,\nu} (-Q_b)^{|\nu|+|\tau|} Q_f^{|\lambda|+|\mu|+|\tau|} f_\tau(q,t)^2\, f_\lambda(t,q) f_\mu(q,t) \qquad (6.4)$$
$$C_{\lambda\nu\emptyset}(t,q)C_{\emptyset\nu^t\mu}(q,t)C_{\tau\emptyset\mu^t}(t,q)T_{\tau^t\lambda^t\emptyset}(t,q)$$

6.4 Example 4

Consider the geometry shown in Fig. 17. In this we have two 4-cycles both of them $\mathbf{P}^2$ joined by a $\mathbf{P}^1$. There are three Kähler parameters (t_{H_1}, t_{H_2}, t_E) corresponding to the curves H_1 (the hyperplane class of $\mathbf{P}^2$), H_2 (the hyperplane class of the second $\mathbf{P}^2$) and the exceptional curve E,

$$Q_{H_i} = \exp(-t_{H_i})\,, \quad Q = \exp(-t_E)\,. \qquad (6.5)$$

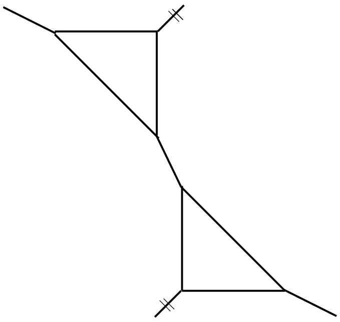

Figure 17. The choice of preferred edges for the geometry with 2 4-cycles.

The partition function of this geometry can be easily determine using the refined vertex and the new vertex. The two horizontal lines we take to be the preferred edges of the refined vertex. Then the refined partition function of this geometry is given by

$$\begin{aligned}Z(Q_{H_1},Q_{H_2},Q) = \sum_{\lambda\,\mu\,\nu\,\sigma\,\eta\,\tau} & (-Q_{H_1})^{|\lambda|+|\mu|+|\nu|}(-Q_{H_2})^{|\sigma|+|\eta|+|\tau|}(-Q)^{|\zeta|} \\ & (f_\nu(q,t)f_\lambda(t,q)f_\mu(q,t)f_\tau(t,q)f_\sigma(q,t)f_\eta(t,q))^2 \\ & C_{\lambda\emptyset\nu}(t,q)C_{\emptyset\mu\nu^t}(q,t)C_{\emptyset\,\sigma^t\tau}(t,q)C_{\eta^t\emptyset\,\tau^t}(q,t)T_{\lambda^t\mu^t\zeta}(t,q)T_{\sigma^t\eta^t\zeta^t}(q,t)\,.\end{aligned}$$

7 Relation with refined Chern-Simons theory

In this section, we will clarify the how the refined Chern-Simons theory [13] is related to the refined vertex and the new vertex.

The refined Chern-Simons theory is formulated as the supersymmetric index of M-theory compactified on $(X \times \mathbb{C}^2) \times_{t,q} S^1$ with N M5-branes on $(L \times \mathbb{C}) \times_{t,q} S^1$, where the fibered product means that

$$\theta \in S^1 \mapsto \theta + 2\pi \implies (z_1, z_2) \mapsto (q\,z_1, t^{-1}z_2)\,,\;\; X \mapsto w(X) \tag{7.1}$$

where w is a $U(1) \times U(1)$ action on X which preserves the holomorphic 3-form and L is a Lagrangian 3-cycle. When $X = T^*S^3$ and $L = S^3$ the large N transition takes the above geometry to resolved coinfold [13, 28].

Consider T^*S^3 with N M5-branes wrapped on S^3 and extending in the z_2-plane along with two stacks of M5-branes wrapped on the Lagrangian cycles $\mathcal{L}_1$ and $\mathcal{L}_2$, which have the topology of $S^1 \times \mathbb{R}^2$, and extending in the z_2-plane. In the S^3 the boundary of these Lagrangian cycles are the two components of the Hopf link. The Lagrangian cycles are shown as dotted line in Fig. 18. Compactifying this brane configuration on circle to go to type IIA string theory we get N D4-branes wrapped on the S^3 with D2-branes ending on these D4-branes giving the open string instantons [25]. Now going through the large N transition the singular geometry, when the S^3 has shrunk, can resolve itself in two different ways related to each other by a flop as shown in Fig. 18.

The normalized open string partition function of the geometry before the transition is then given by [13]

$$\begin{aligned}Z(U_1,U_2) &= \sum_{\lambda\,\mu} Z_{\lambda\,\mu}\, P_\lambda(U_1;q,t)\, P_\mu(U_2;q,t) \qquad (7.2)\\ Z_{\lambda\,\mu} &= P_\lambda(t^{-\rho_N};q,t)P_\mu(t^{-\rho_N}q^{-\lambda};q,t)\,,\end{aligned}$$

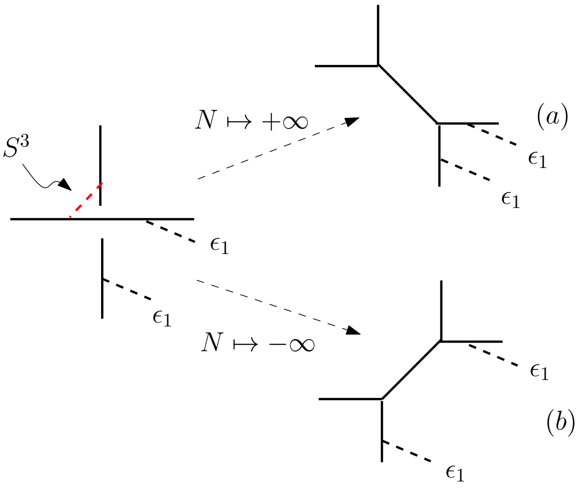

Figure 18. The large N transition can resolve the conifold in two different ways. Resolution given in (a) leads to refined Chern-Simons S-matrix $P_\lambda(t^{-\rho}; q, t)P_\mu(t^{-\rho}q^{-\lambda}; q, t)$ for large N. The resolution of type (b) leads to the refined Hopf link calculated using the refined topological vertex.

where U_1 and U_2 are the holonomies associated with the two branes, $\rho_N = \{-\frac{1}{2}, -\frac{3}{2}, \cdots, -N + \frac{1}{2}\}$ and λ, μ are representations of $SU(N)$. It was shown in [21] that $Z(U_1, U_2)$ is also the partition function of the resolved conifold with branes but taking the Kähler parameter of the resolved conifold $Q = t^{-N}$ so that $N \mapsto \infty$ corresponds $Q \mapsto \infty$. This implies that when large $N \mapsto +\infty$ transition takes the brane configuration to Fig. 18(a) then the large $N \mapsto -\infty$ takes us to Fig. 18(b). Fig. 18(a) gives the refined Chern-Simons Hopf link invariant, $P_\lambda(t^{-\rho_N}; q, t)P_\mu(t^{-\rho_N}q^{-\lambda}; q, t)$, and the Fig. 18(b) gives the refined topological vertex refined Hopf link.

However we can also consider a configuration of branes in which one stack of D4-branes fill the z_1-plane and the other fills the z_2-plane as shown in Fig. 19. In this case the large N transition $N \mapsto +\infty$ shown in Fig. 19(a) gives the refined topological vertex expressed in the basis of Macdonald polynomials.

.

7.1 Local P^2 from refined Chern-Simons Theory

The local $\mathbb{P}^2$ partition function we obtained in section 3 can also be obtained using the refined Chern-Simons theory[6].

In section 3 we showed that slicing of the local $\mathbb{P}^2$ web diagram by ϵ_α branes required a vertex which has ϵ_1 branes on both legs. We obtained this vertex by flop transition from the refined Hopf link. This two-legged vertex is the same as the

---

[6] See [27] for related work.

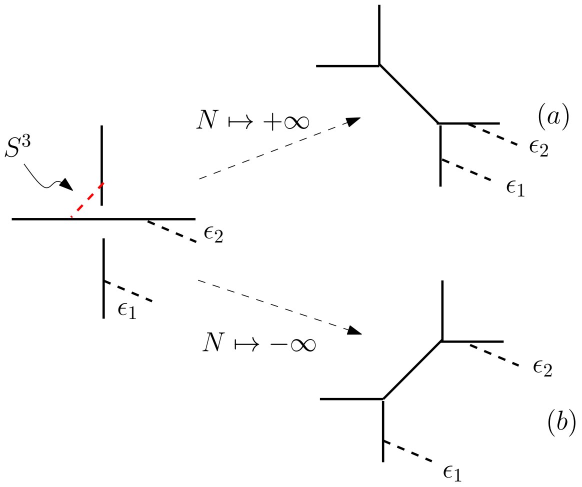

Figure 19. The large N transition with a different configuration of branes.

refined Hopf link S-matrix (in the basis of Schur functions). Thus we can obtain the local $\mathbb{P}^2$ partition function blowing one of the vertices, shrinking the $\mathbb{P}^1$, deforming it to S^3 and putting refined Chern-Simons theory on the S^3 as shown in Fig. 20.

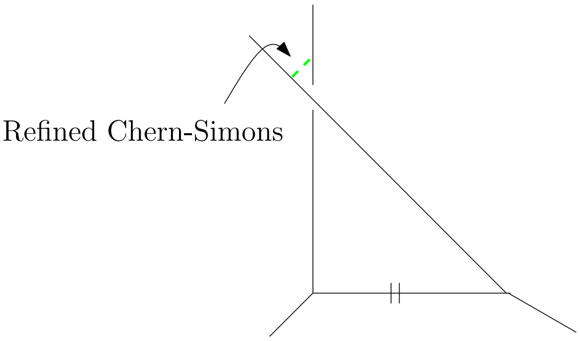

Figure 20. The refined partition function of the blowup of local $\mathbf{P}^2$ can be calculated by putting refined Chern-Simons theory on the S^3. The refined topological vertex is associated with the other two vertices of the geometry. The large N limit then gives the refined partition function of the local $\mathbf{P}^2$.

The local $\mathbb{P}^2$ web diagram can also be sliced in a different way as well. This is shown in Fig. 21. In this case we see that vertices are of the (ϵ_1, ϵ_1), (ϵ_2, ϵ_2) and (ϵ_1, ϵ_2) type[7].

Thus we can write down a different representation of the refined partition func-

---

[7] By a vertex of $(\epsilon_\alpha, \epsilon_\beta)$ type we mean the corresponding branes fill the z_α-plane and the z_β-plane.

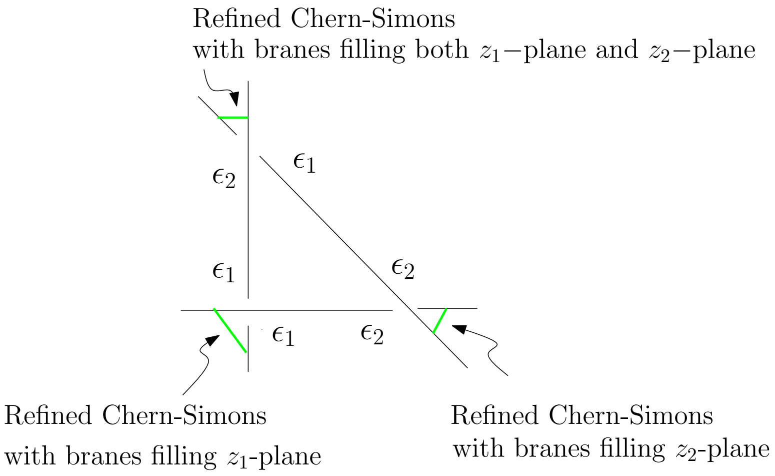

Figure 21. The refined partition function of local $\mathbf{P}^2$ can be obtained from just the refined Chern-Simons theory as well by wrapping appropriate branes on the S^3's and the taking the large N limit.

tion of local $\mathbb{P}^2$:

$$\begin{aligned} Z_{local\,\mathbb{P}^2}(Q,t,q) = \sum_{\nu\,\alpha\,\beta}&(-Q)^{|\lambda|+|\mu|+|\nu|}\left(\frac{t}{q}\right)^{\frac{|\lambda|-|\mu|}{2}} f_\lambda(t,q)f_\mu(t,q)f^2_\nu(q,t) \\ &\Big(P_\lambda(t^{-\rho};q,t)\,P_\mu(t^{-\rho}\,q^{-\lambda};q,t)\Big)\Big(P_\nu(q^{-\rho};t,q)P_{\lambda^t}(q^{-\rho}t^{-\nu})\Big) \\ &\Big[P_{\nu^t}(t^{-\rho};q,t)P_{\mu^t}(q^{-\rho}t^{-\nu};t,q)\Big] \end{aligned} \tag{7.3}$$

The first two factors in second line of the above equation are S-matrices for the refined Chern-Simons theory in which for one of factors $t \leftrightarrow q$. The last factor is different from the first two. The last factor is the refined topological vertex in the basis of Macdonald functions.

8 Conclusions

We have defined a new vertex which can be used along with the refined vertex to calculate the refined partition function of any non-compact toric Calabi-Yau threefold. We believe that this new vertex is closely related to the "index vertex" of Okounkov and Nekrasov [8]. We also showed that refined amplitudes from refined Chern-Simons theory for branes in different z_α-planes can also be calculated from the refined vertex formalism extended by the new vertex.

Acknowledgments

We would like to thank Mina Aganagic, Johannes Walcher and Cumrun Vafa for many useful discussions. We would also like to thank the Simon Center for Geometry and Physics for hospitality during the Simons workshop 2011 where part of this work was carried out. AI was partly supported by the Higher Education Commission grant HEC-2052. CK was partly supported by the INFN Research Project TV12.

9 Appendix A

In this appendix, we sketch the proof that the partition function of the local $\mathbf{P}^2$ computed from the refined vertex Eq. (9.1) and the one from the refined Chern-Simons theory Eq. (7.3) are equal. The section is rather technical and we will try to included all the necessary identities that are used in the manipulations. Let us remind the reader the refined partition function of local $\mathbf{P}^2$:

$$Z_{local\,\mathbf{P}^2} = \sum_{\substack{\lambda\,\mu\,\nu\\ \eta\,\sigma}} (-Q_H)^{|\lambda|+|\mu|+|\nu|}(-1)^{|\lambda|+|\mu|}\left(\frac{t}{q}\right)^{|\lambda|-|\mu|} f_\nu^2(q,t) N^{\eta}_{\lambda\mu} U_{\eta\sigma} f_\sigma P_\sigma(t^{-\rho};q,t) \tag{9.1}$$
$$\times P_{\nu^t}(t^{-\rho};q,t)P_\nu(q^{-\rho};t,q)s_\lambda(t^{-\nu}q^{-\rho})s_\mu(q^{-\rho}t^{-\nu}).$$

First, we want to use the following identity to change the Littlewood-Richardson coefficient to its two parameter extension

$$\sum_{\alpha\,\beta} \widehat{N}^{\sigma}_{\alpha\,\beta} U_{\lambda\,\alpha} U_{\mu\,\beta} = \sum_{\eta} N^{\eta}_{\lambda\,\mu} U_{\eta\,\sigma} \tag{9.2}$$

The reason behind this change becomes obvious when the following non-trivial identity is recalled[8]

$$P_\lambda(t^{-\rho};q,t)P_\mu(t^{-\rho}q^{-\lambda};q,t) = \frac{1}{f_\lambda(t,q)f_\mu(t,q)} \sum_{\nu} \widehat{N}^{\nu}_{\lambda\,\mu} f_\nu(t,q) P_\nu(t^{-\rho};q,t). \tag{9.3}$$

After using this identity, we will have to perform sums of the following form[9]

$$\sum_{\lambda} U_{\lambda\,\alpha} s_\lambda(\gamma\, t^{-\nu} q^{-\rho}), \tag{9.4}$$

---

[8] In [21], this identity played a very crucial role. The definition of the framing factors f_λ differs by a factor of $(-1)^{|\lambda|}$ there, but note that $\widehat{N}^{\nu}_{\lambda\,\mu}$ vanish unless $|\nu| = |\lambda| + |\mu|$, *i.e.*, the identity is also valid when f's are replaced with respect to our current definition of framing factors.

[9] In this section, for brevity of notation, we will use $U_{\lambda\,\mu}$ to mean $U_{\lambda\,\mu}$(q,t) and $\widetilde{U}_{\lambda\,\mu}$ for $\widetilde{U}_{\lambda\,\mu}(t,q)$.

where γ is just a factor. This part gets a little bit more involved, we will need to recall some facts of symmetric functions. There exists an involution which acts on the ring of symmetric functions. In particular, it takes the power sum symmetric function to a multiple of them:

$$\omega \cdot p_n = (-1)^{n-1} p_n. \tag{9.5}$$

One can show that the action of this involution on the Schur functions is less trivial:

$$\omega \cdot s_\lambda = s_{\lambda^t}, \tag{9.6}$$

for all partitions λ. This involution has a two parameter extension $\omega_{t,q}$ which we will use in the following manipulations. Its action on the power sum symmetric function is given by

$$\omega_{t,q} \cdot p_n = (-1)^{n-1} \frac{1-t^n}{1-q^n} p_n, \tag{9.7}$$

for $q, t \neq 1$. In [31], Taki derived an identity using the involution which can be massaged to

$$s_\lambda(\gamma\, q^{-\rho} t^{-\nu}) = \omega_{t,q} \cdot s_{\lambda^t}(-\gamma\, t^{\rho} q^{\nu^t}). \tag{9.8}$$

Using this we can write

$$\begin{aligned} s_\lambda(x) &= \omega_{t,q} \cdot s_{\lambda^t}(x^*) \\ &= \omega_{t,q} \cdot \sum_\eta \widetilde{U}_{\lambda^t\,\eta}\, P_\eta(x^*; t, q) \\ &= \sum_\eta \widetilde{U}_{\lambda^t\,\eta}\, \omega_{t,q} \cdot P_\eta(x^*; t, q) \\ &\equiv \sum_\eta \widetilde{U}_{\lambda^t\,\eta}\, \widehat{P}_\eta(x^*; t, q) \end{aligned} \tag{9.9}$$

where we defined $x = Q_H t^{1/2} q^{-1/2}\, q^{-\rho} t^{-\nu}$ and $x^* = -Q_H t^{1/2} q^{-1/2}\, t^{\rho} q^{\nu^t}$. $\widehat{P}_\eta(x^*; t, q)$ denotes the action of $\omega_{t,q}$ on the Macdonald function. The involution $\omega_{t,q}$ passed through the sum since it acts on the symmetric functions, rather that q, t-dependent factors. Now we are ready to perform the above mentioned sum over λ:

$$\begin{aligned} \sum_\lambda U_{\lambda\,\alpha} s_\lambda(x) &= \sum_{\lambda\,\eta} U_{\lambda\,\alpha} \widetilde{U}_{\lambda^t\,\eta} \widehat{P}_\eta(x^*, t, q) \\ &= \sum_\eta \left(\sum_\lambda \left(\widetilde{U}^{-1}\right)_{\alpha^t\,\lambda^t} \widetilde{U}_{\lambda^t\,\eta} \right) \widehat{P}_\eta(x^*; t, q) \\ &= \widehat{P}_{\alpha^t}(x^*; t, q), \end{aligned} \tag{9.10}$$

where we have used

$$U^T J U = J \implies (U^{-1})_{\alpha\,\beta} = \widetilde{U}_{\beta^t\,\alpha^t}. \tag{9.11}$$

We need to know the action of $\omega_{t,q}$ on the Macdonald function which is given in [23] to be

$$\omega_{t,q} \cdot P_{\alpha^t}(x^*; t, q) = Q_\alpha(x^*; q, t). \tag{9.12}$$

The desired form is obtained by using the following form of the identity Eq. B.29 from [32]

$$Q_\lambda(q^{\nu^t} t^\rho; q, t) = (-1)^{|\lambda|} \left(\frac{t}{q}\right)^{|\lambda|/2} P_{\lambda^t}(t^{-\nu} q^{-\rho}; t, q). \tag{9.13}$$

Using Eq. (9.3) and Eq. (9.10), we can easily show that Eq. (9.1) is equal to Eq. (7.3).

10 Appendix B

In this section, we want to review our notations, conventions and collect some of the useful formulas for the derivations. We want to warn the reader that the convention we follow in this note is different from the one used in [7]. The difference comes from the pictorial representation of the Young diagrams. In [7], for a given representation $\lambda = \{\lambda_1, \lambda_2, \ldots\}$, we illustrated the corresponding Young diagram with columns of height λ_i. The arm length $a(i,j)$ and leg length $\ell(i,j)$ of a given box (i,j) in the diagram were defined as the number of boxes to the right of that box and above that box, respectively. In this note we follow the more conventional notation shown in Fig. 22 where λ_i's are the number of boxes in the i^{th} row. The arm and leg lengths are defined accordingly.

In addition to the arm and leg lengths, we define the co-arm length $a'(i,j)$ and co-leg length $\ell'(i,j)$

$$a(i,j) = \nu_i - j\,, \quad \ell(i,j) = \nu^t_j - i \tag{10.1}$$

$$a'(i,j) = j - 1\,, \quad \ell'(i,j) = i - 1 \tag{10.2}$$

Note that

$$a_\lambda(i,j) = \ell_{\lambda^t}(j,i), \qquad \ell_\lambda(i,j) = a_{\lambda^t}(j,i) \tag{10.3}$$

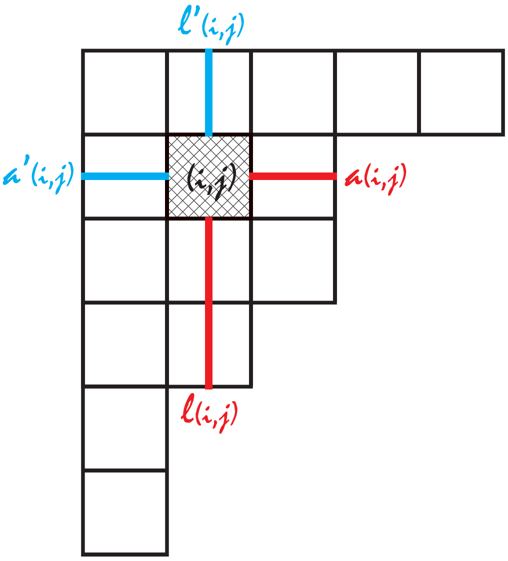

Figure 22. The figure shows the present convention. $\lambda = \{5, 3, 3, 2, 1, 1\}$

with $(i, j) \in \lambda$ and $(j, i) \in \lambda^t$. The difference in the conventions reflects also on some identities used in [7], here we use

$$n(\lambda) = \sum_{i=1}^{\ell(\lambda)} (i-1)\lambda_i = \frac{1}{2}\sum_{i=1}^{\ell(\lambda)} \lambda_i^t(\lambda_i^t - 1) = \sum_{(i,j)\in\lambda} \ell(i,j) = \sum_{(i,j)\in\lambda} \ell'(i,j) = \frac{\|\lambda^t\|^2}{2} - \frac{\lambda}{2} \tag{10.4}$$

$$n(\lambda^t) = \sum_{i=1}^{\ell(\lambda^t)} (i-1)\lambda_i^t = \frac{1}{2}\sum_{i=1}^{\ell(\lambda^t)} \lambda_i(\lambda_i - 1) = \sum_{(i,j)\in\lambda} a(i,j) = \sum_{(i,j)\in\lambda} a'(i,j) = \frac{\|\lambda\|^2}{2} - \frac{\lambda}{2} \tag{10.5}$$

with $\ell(\lambda)$ being the number of non-zero λ_i's, or in other words, it is the number of rows in the Young diagram. The hook length $h(i, j)$ and the content $c(i, j)$ are defined as

$$h(i,j) = a(i,j) + \ell(i,j) + 1, \qquad c(i,j) = j - i \tag{10.6}$$

which satisfy

$$\sum_{(i,j)\in\lambda} h(i,j) = n(\lambda^t) + n(\lambda) + |\lambda|, \tag{10.7}$$

$$\sum_{(i,j)\in\lambda} c(i,j) = n(\lambda^t) - n(\lambda). \tag{10.8}$$

The refined topological vertex in this convention is given by

$$C_{\lambda\,\mu\,\nu}(t,q) = \left(\frac{q}{t}\right)^{\frac{||\mu||^2}{2}} t^{\frac{\kappa(\mu)}{2}}\, q^{\frac{||\nu||^2}{2}}\, \widetilde{Z}_\nu(t,q) \sum_\eta \left(\frac{q}{t}\right)^{\frac{|\eta|+|\lambda|-|\mu|}{2}} s_{\lambda^t/\eta}(t^{-\rho}\, q^{-\nu})\, s_{\mu/\eta}(t^{-\nu^t}\, q^{-\rho}) \tag{10.9}$$

where $s_{\lambda/\eta}(\mathbf{x})$ is the skew-Schur function and $\widetilde{Z}_\nu(t,q)$ is given by

$$\widetilde{Z}_\nu(t,q) = \prod_{(i,j)\in\nu} \left(1 - q^{a(i,j)}\, t^{\ell(i,j)+1}\right)^{-1}, \tag{10.10}$$

which is related to the Macdonald polynomials

$$t^{\frac{\|\nu^t\|^2}{2}}\, \widetilde{Z}_\nu(t,q) = P_\nu(t^{-\rho}; q, t), \tag{10.11}$$

$$q^{\frac{\|\nu\|^2}{2}}\, \widetilde{Z}_{\nu^t}(q,t) = P_{\nu^t}(q^{-\rho}; t, q). \tag{10.12}$$

For the Macdonald polynomials with this special set of argument we have

$$P_\lambda(t^\rho; q, t) = (-1)^{|\lambda|} q^{n(\lambda^t)} t^{-n(\lambda)} P_\lambda(t^{-\rho}; q, t). \tag{10.13}$$

The Macdonald polynomials also satisfy

$$P_\lambda(\mathbf{x}; q, t) = P_\lambda(\mathbf{x}; q^{-1}, t^{-1}) \tag{10.14}$$

For completeness, let us also review some identities regarding to Schur functions and MacDonald polynomials:

$$s_\lambda(\mathbf{x}) s_\mu(\mathbf{x}) = \sum_\eta N^\eta_{\lambda\mu} s_\eta(\mathbf{x}) \tag{10.15}$$

$$s_{\lambda/\mu}(\mathbf{x}) = \sum_\eta N^\lambda_{\mu\eta} s_\eta(\mathbf{x}) \tag{10.16}$$

$$P_\lambda(\mathbf{x}; q, t) P_\mu(\mathbf{x}; q, t) = \sum_\eta \widehat{N}^\eta_{\lambda\mu} P_\eta(\mathbf{x}; q, t) \tag{10.17}$$

$$s_\eta(\mathbf{x}) = \sum_\sigma U_{\eta\sigma} P_\sigma(\mathbf{x}; q, t) \tag{10.18}$$

The following relations among Macdonald polynomials prove to be very useful for our computations

$$\frac{P_\mu(q^{-\lambda}\, t^{-\rho}; q, t)}{P_\mu(t^{-\rho}; q, t)} = \frac{P_\lambda(q^{-\mu}\, t^{-\rho}; q, t)}{P_\lambda(t^{-\rho}; q, t)} \tag{10.19}$$

$$P_\sigma(t^{-\rho}, z\, t^{\rho}; q, t) = P_\sigma(t^{-\rho}; q, t) \prod_{s\in\sigma} (1 - z\, q^{a'(s)}\, t^{-\ell'(s)}) \tag{10.20}$$

The following sum rules are essential for vertex computations

$$\sum_\eta s_{\eta/\lambda}(\mathbf{x}) s_{\eta/\mu}(\mathbf{y}) = \prod_{i,j=1}^{\infty} (1 - x_i y_j)^{-1} \sum_\tau s_{\mu/\tau}(\mathbf{x}) s_{\lambda/\tau}(\mathbf{y}) \tag{10.21}$$

$$\sum_\eta s_{\eta^t/\lambda}(\mathbf{x}) s_{\eta/\mu}(\mathbf{y}) = \prod_{i,j=1}^{\infty} (1 + x_i y_j) \sum_\tau s_{\mu^t/\tau}(\mathbf{x}) s_{\lambda^t/\tau^t}(\mathbf{y}) \tag{10.22}$$

$$\sum_\eta P_\eta(\mathbf{x}; q, t) P_{\eta^t}(\mathbf{x}; t, q) = \prod_{i,j=1}^{\infty} (1 + x_i y_j) \tag{10.23}$$

We have considered the normalized amplitudes, both the open and closed amplitudes are infinite series in the Kähler parameters, however, their ratio is finite as a result of the following identity

$$\prod_{i,j=1}^{\infty} \frac{1 - Q\, q^{-\lambda_i + j - 1/2} t^{i-1/2}}{1 - Q\, q^{j-1/2} t^{i-1/2}} = \prod_{s\in\lambda} \left(1 - Q\sqrt{\frac{t}{q}}\, q^{-a'(s)} t^{\ell(s)}\right). \tag{10.24}$$

References

[1] R. Gopakumar, C. Vafa, "M-Theory and Topological Strings–I", `hep-th/9809187`, R. Gopakumar, C. Vafa, "M-Theory and Topological Strings–II", `hep-th/9812127`.

[2] N. A. Nekrasov, "Seiberg-Witten prepotential from instanton counting," Adv. Theor. Math. Phys. 7 (2004) 831-864, `hep-th/0206161`.

[3] C. Vafa, "Supersymmetric Partition Functions and a String Theory in 4 Dimensions," arXiv:1209.2425 [hep-th].

[4] G. W. Moore, N. Nekrasov and S. Shatashvili, "Integrating over Higgs branches," Commun. Math. Phys. **209**, 97 (2000), `hep-th/9712241`.

[5] T. J. Hollowood, A. Iqbal and C. Vafa, "Matrix models, geometric engineering and elliptic genera," JHEP **0803**, 069 (2008), `hep-th/0310272`.

[6] M. Aganagic, A. Klemm, M. Marino, C. Vafa, "The Topological Vertex," Commun. Math. Phys. 254 (2005) 425-478, `hep-th/0305132`.

[7] A. Iqbal, C. Kozcaz and C. Vafa, "The Refined topological vertex," JHEP **0910**, 069 (2009), `hep-th/0701156`.

[8] A. Okounkov, "Index Vertex", talk at Simon Center for Geometry and Physics, http://scgp.stonybrook.edu/archives/3416.

[9] S. Katz, P. Mayr and C. Vafa, "Mirror symmetry and exact solution of 4-D N=2 gauge theories: 1.," Adv. Theor. Math. Phys. **1**, 53 (1998) [hep-th/9706110].

[10] S. Katz, A. Klemm and C. Vafa, "Geometric engineering of quantum field theories," *Nucl. Phys.* **B497**, (1997) 173–195, `hep-th/9609239`.

[11] H. Nakajima and K. Yoshioka, "Instanton counting on blowup-I, 4 dimensional pure gauge theory," `arXiv:math/0306198 [math.AG]`.

[12] M. Aganagic, M. C. N. Cheng, R. Dijkgraaf, D. Krefl, C. Vafa, "Quantum Geometry of Refined Topological Strings", `arXiv:1105.0630`.

[13] M. Aganagic, S. Shakirov, "Knot Homology from Refined Chern-Simons Theory", `arXiv:1105.5117`.

[14] H. Awata, H. Kanno, "Refined BPS state counting from Nekrasov's formula and Macdonald functions", Int. J. Mod. Phys. A24, 2253-2306, (2009), `arXiv:0805.0191`.

[15] R. Dijkgraaf, C. Vafa, "Toda Theories, Matrix Models, Topological Strings, and N=2 Gauge Systems", `arXiv:0909.2453`.

[16] I. Antoniadis, S. Hohenegger, K.S. Narain, T.R. Taylor, "Deformed Topological Partition Function and Nekrasov Backgrounds", `arXiv:1003.2832`.

[17] D. Krefl, J. Walcher, "Extended Holomorphic Anomaly in Gauge Theory", Lett. Math. Phys. **95**, 67-88, (2011), `arXiv:1007.0263`.

[18] A. Okounkov, N. Reshetikhin and C. Vafa, "Quantum Calabi-Yau and classical crystals," Progr. Math. **244**, 597 (2006) [hep-th/0309208].

[19] R. Dijkgraaf, C. Vafa, E. Verlinde, "M-theory and a topological string duality", `hep-th/0602087`.

[20] S. Gukov, A. Iqbal, C. Kozcaz and C. Vafa, "Link Homologies and the Refined Topological Vertex," Commun. Math. Phys. **298**, 757 (2010), `arXiv:0705.1368 [hep-th]`.

[21] A. Iqbal and C. Kozcaz, "Refined Hopf Link Revisited," JHEP **1204**, 046 (2012) [arXiv:1111.0525 [hep-th]].

[22] H. Awata, H. Kanno, "Macdonald operators and homological invariants of the colored Hopf link", J. Phys. A 44:375201, (2011) `arXiv:0910.0083`.

[23] I. G. Macdonald, "Symmetric functions and Hall polynomials," (second edition, 1995), Oxford Mathematical Monographs, Oxford Science Publications.

[24] B. Eynard, A. -K. Kashani-Poor and O. Marchal, "A Matrix Model for the Topological String I: Deriving the Matrix model," arXiv:1003.1737 [hep-th].

[25] H. Ooguri and C. Vafa, "Knot invariants and topological strings," Nucl. Phys. B **577**, 419 (2000), `hep-th/9912123`.

[26] M. Bershadsky, S. Cecotti, H. Ooguri and C. Vafa, "Kodaira-Spencer theory of gravity and exact results for quantum string amplitudes," Commun. Math. Phys. **165**, 311 (1994), `hep-th/9309140`.

[27] M. Aganagic, S. Shakirov "Refined Chern-Simons and Topological Strings", to appear.

[28] R. Gopakumar and C. Vafa, “On the gauge theory / geometry correspondence,” Adv. Theor. Math. Phys. **3**, 1415 (1999) [hep-th/9811131].

[29] D. R. Morrison and N. Seiberg, “Extremal transitions and five-dimensional supersymmetric field theories,” Nucl. Phys. B **483**, 229 (1997), `hep-th/9609070`.

[30] B. Eynard, C. Kozcaz, ”Mirror of the refined topological vertex from a matrix model”, `arXiv:1107.5181`.

[31] M. Taki, “Flop Invariance of Refined Topological Vertex and Link Homologies,” arXiv:0805.0336 [hep-th].

[32] H. Awata and H. Kanno, “Instanton counting, Macdonald functions and the moduli space of D-branes,” JHEP **0505**, 039 (2005) [hep-th/0502061].